Interactions and Hydration of Nucleic Acid Bases in a Vacuum. Experimental Study

LEONID F. SUKHODUB

Institute for Low Temperature Physics and Engineering, Ukr.SSR Academy of Sciences, Kharkov, USSR

Received December 19, 1986

Contents

Professor Leonid Fiodorovich Sukhodub (born in 1948, Ph.D. in Physics and Mathematics) is a well-known scientist working in the field of experimental biophysics. His current work investigates the thermodynamics of intermolecular interaction in biological complexes, modeling DNA or protein structure. He has published 40 papers and a monograph (to date). At present, Professor Sukhodub is the head of the Biophysical Department at the Institute for Low Temperature Physics and Engineering, Ukr.S.S.R. Academy of Sciences.

I. Introduction

DNA and RNA molecules are substances of heredity in living organisms. Their primary structure is determined by the nucleic acid base sequence along the chain. Higher order structures of biopolymers, which account for their functioning, are formed due to both intermolecular interactions between the monomers and interactions of the monomers with aqueous ion medium.

It is well-known that the main constituent terms of the stabilization energy of the DNA double helix are associated with hydrogen bonding and stacking interactions between the bases. One of the important questions in the problem of DNA stability is the evaluation of the relative contribution of those two factors to the total stabilization energy. This is proved by numerous investigations of interactions on DNA model systems. These investigations, which were performed by the methods of X-ray and neutron diffraction, spectroscopy, etc., have demonstrated that nucleic acid bases in crystals and nonpolar solvents form hydrogen-bonded associates. The thermodynamic parameters of such complexes in nonpolar solvents ($CDCl_3$, CCl_4, etc.) were studied[1-3] by conventional methods (NMR and IR spectroscopy, etc.). The results of these works must be treated as qualitative rather than quantitative due to the solvent effect on base association, which is usually of a considerable value. Poor solubility of bases in nonpolar solvents constituted a significant problem in spectroscopic investigations, which was partly overcome by substantial chemical modification of bases.

In addition to experimental research, a great many theoretical investigations of the structure and stability of H-bonded base complexes in a vacuum have been done (see for review ref 4–6). However, due to the complexity of the systems under investigation, the calculations usually involved different approximations, which led to poor quantitative (and sometimes even qualitative) agreement of the results. The validity of

0009-2665/87/0787-0589$06.50/0

theoretical predictions could not be established due to a complete lack of experimental data obtained under adequate conditions.

It follows therefore that experimental study of the interactions between nucleic acid bases in coplanar and stacking associates under conditions adequate to theoretical models is of great importance and necessity for consistent evaluation of different interaction contributions to the total stabilization energy of the DNA double helix.

The present review includes the results of numerous experimental studies on the thermodynamics of "vacuum" interactions in nucleic acid base associates and in their hydrates, simulating both intermolecular interactions in DNA and interactions of nucleic acid main constituents, bases, with water surroundings.

II. Method of Temperature-Dependent Field Ionization Mass Spectrometry (TD-FIMS)

The quantitative information on weak interactions between nucleic acid bases in a vacuum became available due to the development of temperature-dependent field ionization mass spectrometry (TD-FIMS).[7] This method is based on ionization of molecules in strong electric fields.

A. Theory of Field Ionization

Any atom (molecule), which gets into a strong electric field of the strength $F = 10^7$–10^8 V/cm, is ionized by the mechanism of electron tunneling. The probability of tunneling, Ω, can be approximated according to Wentzel–Kramers–Brillouin[8] as

$$\Omega = \exp\left[-\int_{x_1}^{x_2} \left(\frac{8m_e}{\hbar^2}(E(x) - E_f)\, dx \right)^{1/2} \right] \quad (1)$$

where m_e is the electron mass, E_f is its total energy, and $\hbar$ is Planck's constant. The potential energy $E(x)$ for small values of x can be approximated by the following expression[8]

$$E(x) = \frac{-e^2}{|x_i - x|} + Fex - \frac{e^2}{4x} + \frac{e^2}{x_i - x} \quad (2)$$

in which the first term corresponds to the energy of Coulombic attraction, the second term is the energy of the external electric field, and the third and the fourth terms are the energies associated with the electron and ion images in metal, respectively. The ionization time τ_i at the distance x_i from the metal surface is represented by

$$\tau_i(x) = (\nu\Omega)^{-1} \quad (3)$$

where ν is the frequency of electron "collisions" with the potential barrier. τ_i can be obtained from the following approximate expression[8]

$$\tau_i(x) \approx 10^{-16} \exp(0.68I^{3/2}/F) \quad (4)$$

where I is the ionization potential.

This type of ionization makes it possible to lower molecular fragmentation substantially, since electron tunneling does not cause a transition of the resulting ion to a highly excited energy state. Thus it becomes possible to obtain mass spectra of relatively complex organic and biological compounds[9,10] and also to investigate, as it will be shown later, the association energy of biomolecules in a vacuum. The mechanism of field ionization is discussed in more detail elsewhere.[11]

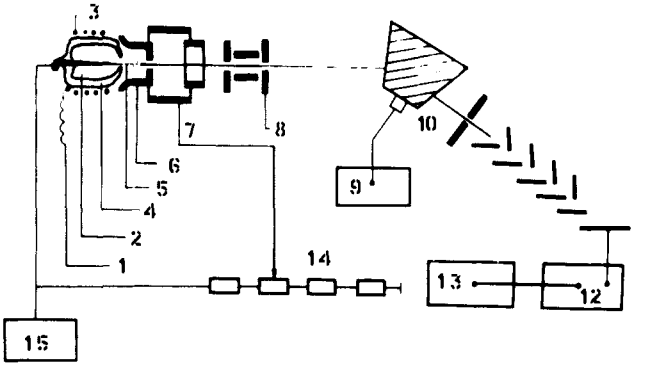

Figure 1. Instrumental arrangement of the FI mass spectrometer: (1) thermocouple; (2) the compound under investigation; (3) heater; (4) evaporator; (5) emitter; (6) counter electrode; (7) focusing lenses; (8) output slit; (9) field-strength meter; (10) magnet; (11) multiplier; (12) amplifier; (13) recorder; (14) voltage divider; (15) accelerating voltage unit.

B. Instrumental Technique

Figure 1 shows the instrumental arrangement for TD-FIMS, constructed on the basis of a MI model mass spectrometer ("Electron" Plant, USSR)[12,13] by using previous designs, made at the Institute of Chemical Physics of the Ukr.SSR Academy of Sciences. The specific element of the ion source is a Knudsen evaporator, combined with the field ionization tip emitter. The temperature of the evaporator with a substance (or a mixture of substances) was monitored by a differential copper–constantan thermocouple. The ionic beam was focused by a set of cylindrical lenses. The operating potential of the emitter was U_e = 1–4 kV, that of the counter electrode U_{ce} = –(0–6) kV, and that of the focusing lenses $U_f = {}^1/_2U_e$. The mass spectrometer made it possible to measure (a) enthalpies of biomolecule association in a vacuum, (b) sublimation heats of biomolecular crystals, and (c) adiabatic ionization potentials (I) of biomolecules.

III. Interactions between Nucleic Acid Bases in a Vacuum

By use of the new method of TD-FIMS, nucleic acid base complexes were observed in a vacuum for the first time.[7,12] They appear due to the existence of high molecular density near the emitter, which is sufficient to cause a considerable number of collisions between the molecules. The zone of high density is formed by the action of an attractive force, applied to the molecules, that is oriented toward the emitter and equal to the polarization energy gradient E_{pol} of the molecule in the field F.

A. Analysis of Thermodynamic Equilibrium Conditions

The formation of base complexes can occur only in close vicinity to the tip surface, where the molecular concentration is high enough to provide a noticeable level of collisions between the molecules.[14] The emitter surface may catalyze the association reactions, but this does not alter the equilibrium concentrations of inter-

acting molecules since catalysis can change only reaction rates, not equilibrium conditions.

Achievement of thermodynamic equilibrium requires the time of its establishment, τ', to be much smaller than the time τ_i, during which molecules are in a nonionized state at the emitter. In the case of 9MeAde with an ionization potential I = 7–9 eV,[15] eq 4 yields $\tau_i \approx 10^{-6}$ s. The electric field strength was calculated by using an approximate equation $F_e = U_e/5r_e$,[8] with U_e = 3 kV and the radius of the tip curvature, r_e, ~ 1000 Å. The collision relaxation time is related to the mean molecule lifetime between two collisions, which is equal to

$$\tau' = \frac{1}{\bar{v}} = \frac{1}{n\sigma_c}\left(\frac{m}{3kT}\right) \quad (5)$$

where $\bar{v}$ is the mean thermal velocity and σ_c is the collision cross section. With the molecular diameter of about 3 Å ($\sigma_c = 3 \times 10^{-5}$ cm^2) and T = 300 K, one estimates $\tau' \approx 10^{-11}$ s. Thus it is clear that molecules undergo numerous collisions prior to ionization, leading to the establishment of thermodynamic equilibrium in the system.

It should be noted that the ions are removed from the surface layer during the time τ'', which can be estimated as

$$\tau'' \sim [mh^2/(2eU_e)]^{1/2} \quad (6)$$

and equals by an order of magnitude 10^{12}–10^{13} s if the layer thickness at the emitter is $h \sim 10$ Å. It follows that under the experimental conditions ion–molecular reactions can be neglected.

In summary, the relation between characteristic time intervals is given by

$$\tau'' < \tau' \ll \tau_i \quad (7)$$

B. Evaluation of Thermodynamic Parameters

Peak intensities in mass spectra are related to the molecular concentration in the ionization zone as[14,16]

$$I_x(F) = \sigma_x(F)n_x(F) \quad (8)$$

where $I_x(F)$ is the peak intensity for molecule x at field strength F, $\sigma_x(F)$ is the ionization coefficient, and $n_x(F)$ is the concentration of neutral molecules. Similarly, for a dimer xy, which is produced by the reaction x + y $\rightleftharpoons$ xy, one has

$$I_{xy}(F) = \sigma_{xy}(F)n_{xy}(F) \quad (9)$$

Under equilibrium conditions $n_{xy}/n_x n_y = K_{assc}^{real}$, where K_{assc}^{real} is the association constant, related to the reaction enthalpy ΔH_{assc} by the equation

$$\ln K_{assc}^{real} = -\Delta H_{assc}/RT \quad (10)$$

The value of K_{assc} for the above-mentioned reaction can be calculated from mass spectrometric data by using eq 8 and 9

$$K_{assc}^{xy} = I_{xy}/I_x I_y \quad (11)$$

Thus the relation between K_{assc} and K_{assc}^{real} is given by

$$K_{assc}^{real} = K_{assc}\frac{\sigma_{xy}(F)}{\sigma_x(F)\cdot\sigma_y(F)} = K_{assc}\sigma^*(F) \quad (12)$$

Generally speaking, coefficient $\sigma^*(F)$ may depend on temperature. However, this dependence can be neglected in the temperature range employed in the measurements of ΔH_{assc} since sublimation heats obtained from mass spectrometric data are in good agreement with those measured by the low-temperature quartz resonator method.[14]

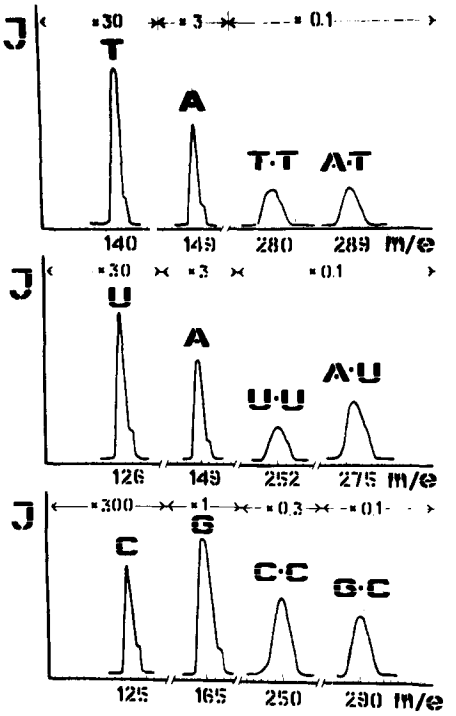

Figure 2. FI mass spectra for the mixtures Ade + Thy, Ade + Ura, and Gua + Cyt.

C. Coplanar H-Bonded Complexes

To observe Watson–Crick pairs in a vacuum, the following purine–pyrimidine mixtures were used: 9MeAde + 1MeThy, 9MeAde + 1MeUra, and 9MeGua + 1MeCyt. Figure 2 shows the sections of FI mass spectra of these mixtures that correspond to molecular ions of pyrimidine, T^+, U^+, and C^+, and purine, A^+ and G^+, bases and their homo- and heterocomplexes, TT^+, UU^+, and CC^+ and AT^+, AU^+, and GC^+. The formation of complex ions comprises (1) the formation of neutral complexes and (2) their ionization. It was suggested that bases in a dimer are bonded by H-bonds similar to the case of dimers in nonpolar solvents. To prove this suggestion we have studied the mass spectrum of a mixture of 1MeUra + 1,3MeUra + 1,3MeThy. Since 1,3MeUra and 1,3MeThy molecules cannot form H bonds $2M^+$ peaks must be absent in their mass spectra, which was the case.[13] Thus it becomes clear that base dimers observed in the mass spectra are hydrogen bonded (Figure 2).

Temperature dependences of the FI mass spectra of base mixtures were recorded, and the data plotted as ln K_{assc} vs. $f(1/T)$ gave straight lines for 9MeAde·1MeUra, 9MeAde·1MeThy, and 9MeGua·1MeCyt pairs. Similar dependences were obtained for other pairs. From the slope of the lines enthalpies were derived (Figure 3) and are listed in Table I.

In order to further confirm that the enthalpy values were obtained by FIMS under thermodynamic equilibrium conditions, ΔH_{assc} of 1,3MeUra·1,3MeUra dimers was measured by IR spectroscopy.[16] A metal cell with sapphire windows was used, with a 1600-cm^{-1} lower

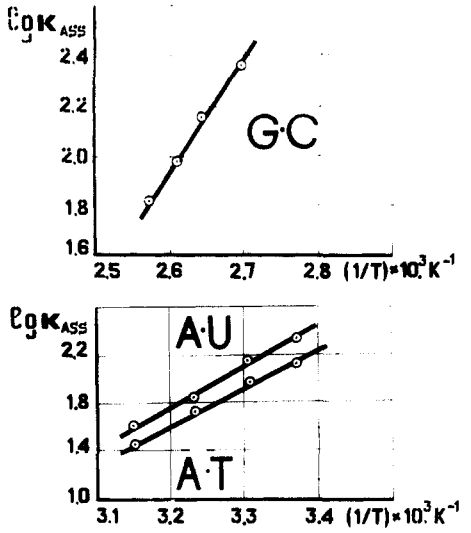

Figure 3. Variation of K_{assc} with temperature for the pairs Ade·Ura, Ade·Thy, and Gua·Cyt.

TABLE I. Energies of H-Bonded Nucleic Acid Base Dimers (kcal/mol)

	exptl $-\Delta H$		theor - E		
dimer	in a vacuum	in $CDCl_3$ [1]	[26]	[17]	[27]
Ade·Ura	14.5	6.2		13.5	11.9
Ade·Thy	13.0		11.46	13.6	
Gua·Cyt	21.0	10.0–11.5	24.42	23.7	25.5
Ura·Ura	9.5	4.3		10.1	9.7
Thy·Thy	9.0			9.5	
Cyt·Cyt	17.5	6.3		20.3	17.5

limit of transmission range. The cell with the investigated substance was pumped out to the pressure of $\sim 10^{-4}$ Torr and placed into a furnace. The measurements were performed by using a single-beam vacuum IRS-3I spectrophotometer (USSR). At temperatures higher than 508 K the IR spectrum shows not only the NH monomer absorption band at $\nu_{NH} = 3445$ cm^{-1} but also a band at $\nu = 3225$ cm^{-1}, which corresponds to vibrations of H-bonded NH groups. In the temperature range 548–570 K an antibate dependence of the monomer and dimer absorption bands is observed, from which the enthalpy of association $\Delta H_{assc} = 9.2 \pm 0.9$ kcal/mol was derived, in good agreement with ΔH_{assc} obtained by TD-FIMS (Table I).

D. Effect of the Field Strength

Nucleic acid base molecules interact with external electric field F due to their polar nature. As a result both molecules in a complex will tend to orient with their dipole moments $\vec{\mu}$ parallel to the external field $\vec{F}$. Therefore if in the absence of the external field molecular dipoles in the complex of optimum configuration are not parallel, one can expect a stretching effect of the external field, which will cause a decrease of the interaction energy in the complex. In this connection temperature dependences of K_{assc} for all the investigated pairs (except for the 9MeGua·1MeCyt pair, which shows a weak GC^+ peak)[16] were studied at different emitter potentials, $U_e = 1.3$–3 kV. In the case of Ade·Thy, Ade·Ura, Ura·Ura, and Thy·Thy pairs, no dependence of ΔH_{assc} on F was observed, while the enthalpy of the reaction Cyt + Cyt $\rightleftharpoons$ Cyt·Cyt decreased noticeably from $\Delta H^{CC} = -9.6$ kcal/mol ($U_e = 3$ kV) to $\Delta H^{CC} = -17.06$ kcal/mol ($U_e = 1.3$ kV), which is probably due to a larger dipole moment of Cyt as compared to other bases[15] and also to a less favorable mutual orientation of the dipoles in the dimer. The value of $\Delta H^{CC} = -17.5$ kcal/mol for the Cyt·Cyt pair in Table I was obtained by extrapolation of the ΔH vs. U_e plot to zero field ($U_e = 0$).

The results on field dependences qualitatively agree with recent theoretical calculations of interaction energies in Ade, Gua, Thy, Ura, and Cyt H-bonded dimers in electric field F.[18] These calculations were performed by using the following representation of the total interaction energy between two base molecules in field F:

$$E_{1,2}{}^F = E_{el}{}^F + E_{dis} + E_{pol}{}^F + E_{rep} \qquad (13)$$

Interaction with the field was allowed for by varying $E_{el}{}^F$ and $E_{pol}{}^F$. In the case of electrostatic energy $E_{el}{}^F$ an additional term was introduced, which corresponded to the interaction of the dimer dipole moment with the field F:

$$E_{el}{}^F = E_{el} - (\vec{\mu}_{(1)} + \vec{\mu}_{(2)})\vec{F} \qquad (14)$$

The polarization term $E_{pol}{}^F$ of $E_{1,2}{}^F$ was calculated as a sum of polarization energies of each molecule $E_{pol}{}^{F(m)}$. The latter was obtained with regard to the external field by using the formula

$$E_{pol}{}^{F(m)} = -\tfrac{1}{2}\sum_i{}^{(m)}\alpha_i(\vec{\epsilon}_i + \vec{F})^2 \qquad (15)$$

where $\vec{\epsilon}_i$ is the electric field at point i of molecule 1, induced by the charge distribution of molecule 2, and

$$\sum_i{}^{(m)}\alpha_i = \alpha^m$$

is the total molecular polarizability of bases.

The interaction (stabilization) energy of two base molecules in field F is given by

$$\Delta E_{1,2}{}^F = E_{1,2}{}^F - (E_1{}^F + E_2{}^F) \qquad (16)$$

Analysis of $\Delta F_{1,2}{}^F$ values revealed that the strong field dependence of the stabilization energy is characteristic of Gua·Cyt and Cyt·Cyt dimers, which agrees qualitatively with the experimental results for Cyt·Cyt dimer. At the same time a noticeable quantitative disagreement should be pointed out: the theory predicts a great association energy decrease with increasing F. We consider this to be due to consideration of an overly simplified theoretical model,[18] which did not allow for interaction of biomolecules with the emitter surface, the interaction energy being $E_1 \sim e^2/r$ (r is the distance between a molecule and its image in metal). At the same time E_1 for bases is of the same order of magnitude as $E_2 \sim \vec{\mu}\vec{F}$, which is connected with molecule orientation along the field. This fact necessitates theoretical calculations.

When one takes into consideration the independence of ΔH values on the ionization field F for most of the complexes, it can be concluded that the reaction system is in thermodynamic equilibrium, that is, the inequality $\tau' \ll \tau_i$ is valid in the whole range of U_e values. At the same time the observed field effect for Cyt·Cyt dimer shows that when thermodynamic parameters of molecular associates are measured by the TD-FIMS method, the possibility of the electric field effect on the measured values of K_{assc} and ΔH should be investigated and, if observed, ΔH vs. F plots should be extrapolated to zero field.

TABLE II. Energies of Stacking Nucleic Acid Base Dimers in a Vacuum (kcal/mol)

dimer	$-\Delta H^a$	$-E(1)$	$-E(II)$	$-E_{vdv}^{(II)}$	$-E_{Coul}^{(II)}$	$-E_2$	$-E^{27}$	$-E^{17}$
Ura·Ura	5.5						6.7	8.9
1,3MeU·1,3MeU	8.7	8.04	8.11	5.42	2.70	1.8		
Thy·Thy	7.2						7.1	8.9
1,3MeT·1,3MeT	10.4	8.41	8.46	7.01	1.45	0.5		
Cyt·Cyt	7.7						12.2	13.6
1,4,4MeC·1,4,4MeC	12.5	14.26	15.22	6.83	8.4	5.1		
Ade·Ade	4.3	7.0					7.7	7.4
6,6,9MeA·6,6,9MeA	9.1	11.10	11.39	8.70	2.69	4.7		
Coff·Coff	11.9						12.3	14.6
2,2,9MeG·2,2,9MeG		14.33	15.00	8.37	6.63			

[a] Estimations are given for energies of canonical base dimers.

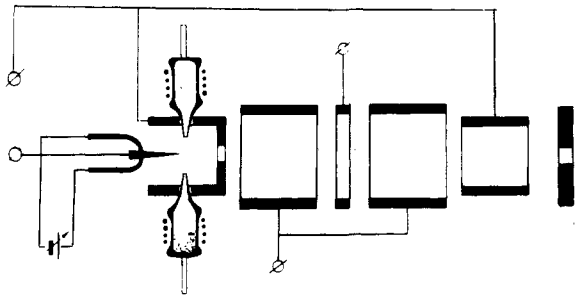

Figure 4. FI ion source with independent heating of two evaporators and a tip emitter.

E. Stacking Dimers of Completely Methylated Bases

TD-FIMS was also used to evaluate enthalpies of formation of base stacking dimers in a vacuum.[19] According to theory[4,5] the main contribution to the stabilization energy of these complexes is associated with dispersion interactions E_{dis}. Bases methylated at all proton-donor sites were used, which could not build up complexes through hydrogen bonding. A more sensitive mass spectrometer was used, designed on the basis of the latest Model MI-1201 mass spectrometer ("Electron" Plant, USSR). The instrument was supplied by a modified FI ion source (Figure 4), in which two evaporators and the tip emitter could be heated independently.

As an example, Figure 5 shows typical FI mass spectra of completely methylated Ade (6,6,9MeAde) and Cyt (1,4,4MeCyt). $2M^+$ peaks are observed, which correspond to stacking dimers. To obtain ΔH values, temperature dependences of the ionic currents I were taken, which corresponded to monomer component (M^+) and to the resulting dimers ($2M^+$). Figure 6 shows typical $\lg I - f(i_e)$ dependences for 6,6,9MeAde (i_e being the current through the emitter arc). For every point of the $\lg I - f(i_e)$ plots the values of K_{assc} were calculated, and from their temperature dependences ΔH values were obtained (Table II).

Since the dimerization reactions occur in a strong electric field, measurements of ΔH for all complexes were performed at different emitter potentials. Of particular interest are these measurements for Cyt, since in the case of the H-bonded Cyt·Cyt complex a noticeable field effect on ΔH was observed.

In the case of a 1,4,4MeCyt dimer ΔH values also show dependence on F, though a weaker one as compared to the H-bonded dimer: at emitter potentials of 3, 4, and 5 kV the corresponding ΔH values were 12.0, 11.5, and 10.6 kcal/mol. The value of ΔH = 12.5 kcal/mol in Table II was obtained by extrapolation of the ΔH vs. U_e plot to zero field. Methyl derivatives of Ade and Thy showed no field dependences. In the case of 1,3MeUra and coffein such measurements could not be done owing to very weak $2M^+$ peaks in the original FI mass spectra of these compounds.

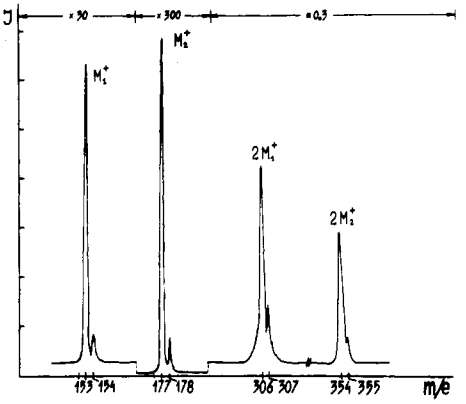

Figure 5. FI mass spectrum of the mixture of triply methylated Cyt (M_1^+) and Ade (M_2^+). $2M_1^+$ and $2M_2^+$ peaks arise from stacking dimers.

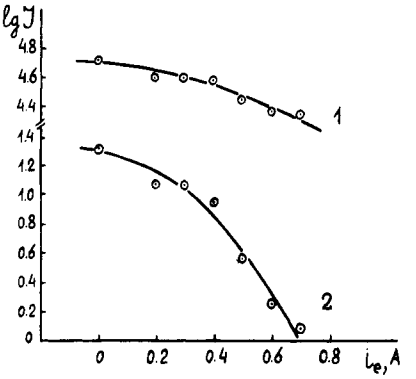

Figure 6. Variation of $\lg I_m$ (curve 1) and of $\lg I_{2M}$ (curve 2) with i_e for 6,6,9MeAde.

To obtain some structural information for dimers of base methyl derivatives in a vacuum, calculations were performed by using the method of atom–atom potential functions.[6] Molecules were treated both in the perfectly rigid body approximation and in a model with conformational degrees of freedom. Base geometry was taken from X-ray data.[20] Substituents at NH_2 groups in the rigid body model were supposed to lie in the molecule plane, and the orientation of methyl groups was chosen in which the H atom, lying in the molecule plane, was oriented toward the most negatively charged nearest-neighbor atom. In the model with conformational de-

grees of freedom methyl and amino groups were free to rotate. Interaction between atoms of the same molecules was not considered.

The calculation was performed by using the Lennard-Jones potential:

$$\varphi_{ij} = q_i q_j r_{ij}^{-1} - A r_{ij}^{-6} + B r_{ij}^{-12} \qquad (17)$$

Potential parameters and atomic charges were taken from ref 21 and 22. The potential energy minimum was found by using the methods of the quickest descent and of ravines for the local and the global search, respectively.[23] The full search that was performed in a perfectly rigid body approximation by using six degrees of freedom for one molecule of the complex allowed an estimation of the location of some minima. Subsequent local minimization gave the exact values of coordinates and depths of the main minima for all the complexes.

In the case of the model with conformational degrees of freedom the dimensionality of the minimization space increased to 14, 12, and 10 for methyl derivatives of Ade, Gua, and Cyt, Thy, and Ura, respectively. In order to simplify the computations, local minimization was done only for the deepest minima, obtained through the full search procedure in the perfectly rigid body approximation, which did not alter the position of the global minimum significantly. In addition, for bases containing NH_2 groups a full search was done, which did not reveal any additional minima. The results of calculations for both models are listed in Table II. The structures of the complexes, which correspond to global minima in the model with conformational degrees of freedom, are shown in Figure 7. It should be noted that for each complex a few local minima exist, which differ from the global minimum by less than 0.5 kcal/mol. The computations were done on an ES-1033 computer using ALGOL-68 language (A68LSU translator).[24]

F. Discussion of the Results and Comparison with Theory

Inspection of the data on coplanar dimers (Table I) shows that Ade·Thy, Ade·Ura, and Gua·Cyt Watson–Crick pairs are noticeably energetically more favorable than corresponding homodimers. This substantiates the suggestion[20] about electronic complementarity of the bases that form Watson–Crick pairs. The results are also in qualitative agreement with those of quantum mechanical calculations done before 1979 and reviewed in ref 4 and 5. A comparison with the results of recent theoretical calculations[17,25-27] gives a satisfactory quantitative agreement between predicted energy values and those measured by the TD-FIMS method (Table I), the agreement being almost the same in the case of the most complicated methods of calculation,[17] dealing with a multipole charge distribution that was obtained with ab initio wave functions, and in the case of a much simpler method of atom–atom potential functions with a 1-10-12 potential for interaction through hydrogen bonding between N–H and O(N) groups or by a 1-6-12 potential for all other interactions.[27]

These results elucidate solvent effects on complex formation: in the case of $CDCl_3$ interaction energies in complexes are about 2 times lower as compared to the vacuum values (Table I). This effect can be explained as follows. Association of molecules in nonpolar solvents causes a considerable energy loss in solvent–base (ΔE_{s-b}) and solvent–solvent (ΔE_{s-s}) subsystems. This follows from the results of direct Monte Carlo calculations of complex formation for Ade·Ura and Gua·Cyt pairs in a nonpolar solvent CCl_4, which was approximated by 175 CCl_4 molecules placed in a parallelepiped 38.02 × 27.14 × 27.14 Å by measure.[25] The total energy of complex formation ΔE_c was calculated as

$$\Delta E_c = \Delta E_{s-s} + \Delta E_{s-b} + \Delta E_{b-b} \qquad (18)$$

It was shown that in CCl_4 ΔE_c values for H-bonded Ade·Ura and Gua·Cyt dimers were equal to −6.3 and

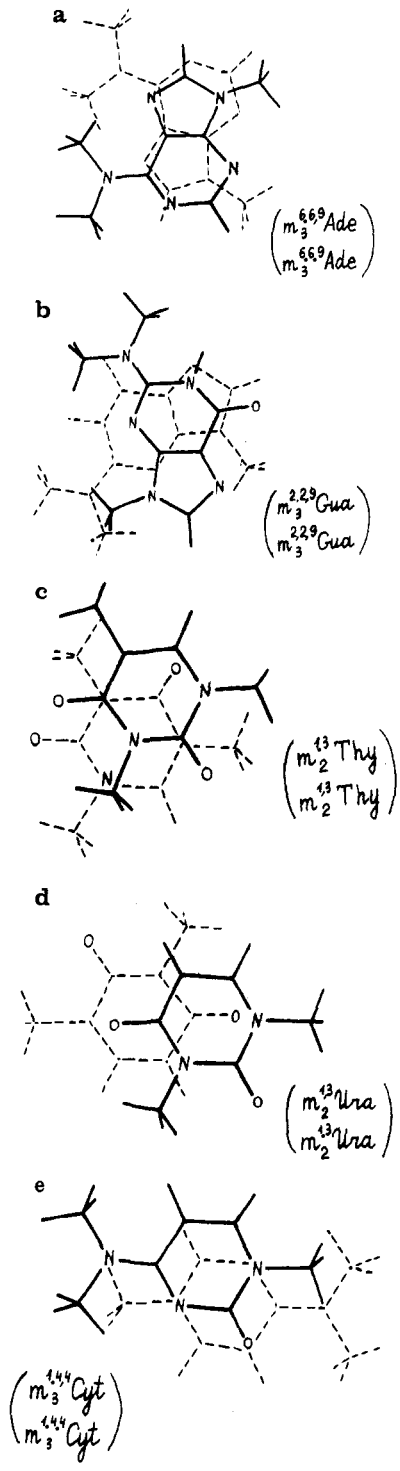

Figure 7. Global minimum energy configurations of complexes: (a) 6,6,9MeAde; (b) 2,2,9MeGua; (c) 1,3MeThy; (d) 1,3MeUra; (e) 1,4,4MeCyt.

−17.6 kcal/mol, respectively. At the same time changes of the components ΔE_{s-b} and ΔE_{s-s} were of almost the same value: ΔE_{s-b} = 2.2 and 2.3 kcal/mol; ΔE_{s-s} = 4.1 and 3.8 kcal/mol. These results show that formation of an H-bonded dimer causes only minor changes in a solvent–base subsystem, since the main contribution to interaction between nonpolar CCl_4 molecules and planar bases is associated with dispersion forces.[4,5] Such interaction implies "vertical" configuration of the interacting molecules; i.e., CCl_4 molecules are situated above and under the aromatic plane, thus not interfering with the formation of hydrogen bonds. The relative stability of H-bonded base pairs in a vacuum is as follows:

$$\text{Gua·Cyt} \gg \text{Cyt·Cyt} > \text{Ade·Ura} > \text{Ade·Thy} > \text{Ura·Ura} > \text{Thy·Thy} \quad (19)$$

Analysis of stacking base dimer energies in a vacuum (Table II) reveals the following.

The theoretical value of the dimer potential energy E is related to the enthalpy ΔH of the reaction M + M $\rightleftharpoons$ 2M by the equation

$$\Delta H = E + 4RT + E_2^{2M} + 2(E_1^{2M} - E_1^{M}) \quad (20)$$

where E_1 and E_2 are energies of intra- and intermolecular vibrations, respectively. The force field of the complex has, obviously, a weak effect upon intermolecular vibrations; therefore, the term $2(E_1^{2M} - E_1^{M})$ is small as compared to the other terms of eq 20 and can be neglected. Thus the expression for energies of intermolecular vibrations in the complex is given by

$$E_2^{2M} = \Delta H - E - 4RT \quad (21)$$

An analysis of E_1^{2M} values reveals an anomalously low energy of intermolecular vibrations for the 1,3MeThy dimer as compared to other complexes (Table II). It is due, probably, to the structure of this complex (a close proximity of methyl and carbonyl groups) on one hand, and to a large number of methyl groups that impede intermolecular vibrations, on the other. As for the structures of other associates, it should be pointed out that in the case of dimethyluracil the predicted configuration (Figure 7) is similar in many respects to those of Ura[17,27] and 1,3MeUra dimers,[18] the only difference being a smaller overlap of molecular backbones, which probably results in an appreciable contribution to E_2 of the 1,3MeUra dimer as compared to the 1,3MeThy dimer (Table II). Other structures of methylated base dimers also differ from optimal configurations for canonical bases, the loss in the stabilization energy being, however, small due to the presence of a few local minima with almost the same energy. At the same time methylation of bases results in an increase of the number of interacting groups, which in turn leads to an increase in the stabilization energy of stacking dimers in a vacuum. Therefore the stabilization energy of methylated base dimers should be greater than that of canonical stacking dimers. A comparison of experimental enthalpies for 1,3MeUra and 1,3MeThy dimers with theoretical data for Ura, 1,3MeUra, Ade, and 6,6,9MeAde dimers (Table II) supports this assumption. A quantitative analysis of the results presented above indicates that an additional stabilization energy of 0.7–0.8 kcal/mol is associated with each methyl group in a complex. Assuming that methyl groups contribute about the same to the stabilization energy of the 1,4MeCyt dimer, it is possible to estimate enthalpies of canonical base stacking dimers in a vacuum (Table II). These values are in the best qualitative agreement with the theoretical results of Poltev et al.,[27] obtained by the method of atom–atom potential functions. The only exception is Cyt dimer; in this case the theoretical value[27] markedly exceeds the experimental one (Table II).

A comparison of experimental values of stacking and hydrogen-bonded dimer enthalpies suggests that coplanar interactions between bases make a much greater contribution to DNA stabilization energy as compared to the stacking interactions.

IV. Hydration of Nucleic Acid Bases in a Vacuum

It is well-known that hydration of nucleic acids plays a crucial role in the determination of their conformational properties, which are of importance for their interaction with proteins and solvent molecules. However, until recently our knowledge of nucleic acid constituent hydration was restricted to quantum mechanical and atom–atom calculations.[28-39,49] Experimental data on interaction energies of isolated nitrogen bases with water molecules in a vacuum became available due to development of TD-FIMS.

A. Enthalpies of Water Clusters

Association of water molecules under FI conditions was observed and investigated in a number of works.[40-43] However, none of these works, with the exception of ref 40, dealt with thermodynamic properties of the complexes, whereas such data are of great interest both for the problem of biomolecular hydration and for the development of an up-to-date theory of water structure and description of its macroscopic properties at the molecular level.

At this time theory provides numerous data concerning the energetics and geometry of small water clusters.[44-48] However, systematic experimental investigations of water association energies under conditions adequate to theoretical models have not been done yet, since a proper method was absent.

Here we present experimental and theoretical data on enthalpies of small water cluster $(H_2O)_n$ (n = 2–6) formation in a vacuum.[50,51] The calculations have been done by using the data on normal vibration frequencies of complexes[52] and potential energies of their formation.[44]

Water complexes were obtained by supplying water vapor to the tip emitter from a glass evaporator (Figure 4), which contained crystallohydrate $CuSO_4·5H_2O$. Owing to the effect of field condensation, a zone with high density of H_2O molecules was formed in the vicinity of the tip surface, where molecular collisions occurred with noticeable frequency. The degree of association depended substantially on the material of the tip; e.g., if a platinum tip was used instead of a tungsten one, the proportion of $(H_2O)_n$ complexes with $n > 3$ decreased drastically, which indicated that complexes were formed preferentially in the gas phase. Temperature effect on FI mass spectra was studied by passing an electric current through a metal arch fastened to the emitter. The temperature was monitored by a differential copper–constantan thermocouple,

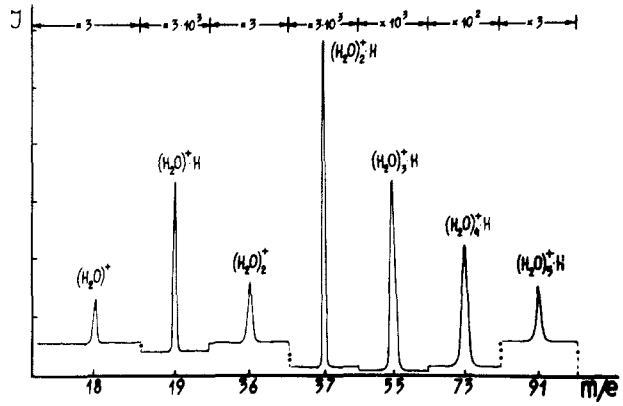

Figure 8. FI mass spectrum of water, registered with a tungsten emitter at 298 K. Peak intensities should be multiplied as indicated.

which was glued to the metal arch in close vicinity to the tip.

1. Experimental Results

The original FI mass spectrum of water, recorded at emitter temperature T_e = 298 K (Figure 8), shows a set of peaks for complex ions $(H_2O)_{n-1}H^+$ (n = 2–6), which were formed by the following mechanism. Neutral clusters $(H_2O)_n$ (n = 2–6), stabilized by O–H...O hydrogen bonds, were formed, and then some of them were ionized by tunneling into the metal of an electron from the oxygen atom, which participated in the O_i–H...O_j hydrogen bond. Redistribution of the electron density in the three-atom system resulted in proton transfer from the O_i atom to the O_j atom followed by detachment of the OH group from the cluster:

$$(H_2O)_{n-1} + H_2O \rightleftharpoons (H_2O)_n \xrightarrow{\text{ionization}} (H_2O)_{n-1}^+ + OH + e^- \rightarrow (H_2O)_n^+ \quad (22)$$

The peak at m/e 36 (Figure 8) indicates that the ionization mechanism of some complexes does not involve proton transfer.

Since peak intensities in the mass spectra are proportional to concentrations of particles that interact at the tip, it is possible to obtain apparent association constants K_{assc} from the reagent and complex peak intensities, while from temperature dependences of K_{assc} enthalpy values can be derived.

In the case of small clusters $(H_2O)_2$ and $(H_2O)_3$, K_{assc} values were obtained from the unambiguous equations for the following reactions

$$H_2O + H_2O \rightleftharpoons (H_2O)_2; \qquad (H_2O)_2 + (H_2O) \rightleftharpoons (H_2O)_3 \quad (23)$$

From H_3O^+, $(H_2O)_2^+$, and $(H_2O)_2^+H$ ion intensities

$$K_{assc}^{(H_2O)_2} = \frac{I_{(H_2O)_2^+}}{(I_{H_3O^+})^2}; \qquad K_{assc}^{(H_2O)_3} = \frac{I_{(H_2O)_2^+H}}{(I_{H_3O^+})^2} \quad (24)$$

Collisions between three particles were not considered because of their extremely low probability. Instead of a low H_2O^+ peak intensity, H_3O^+ peak intensity was substituted in eq 24 since it was found experimentally that $I_{H_2O^+} \sim I_{H_3O^+}$.

By use of the values of K_{assc} calculated for different points of lg I_i vs. i_e plots (Figure 9) for reagent and

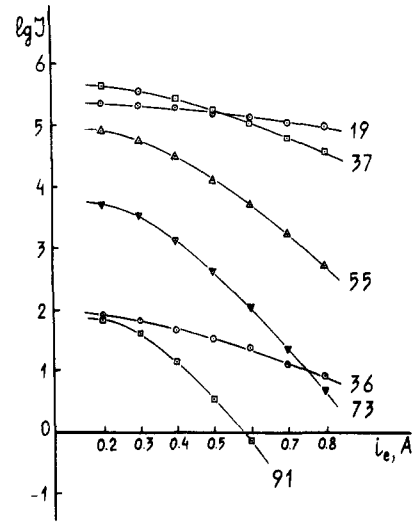

Figure 9. Variation of ionic currents $I_{(H_2O)^+H}$ with temperature (i_e is the electric current through the emitter). Numbers at the curves are the m/e values for the corresponding ions.

complex ions, van Hoff's dependences lg $K_{assc} - f(1/T)$ were plotted and reaction enthalpies $\Delta H_{assc}{}^2$ and $\Delta H_{assc}{}^3$ were calculated. To obtain enthalpies for higher polymers the most probable reaction pathways were considered:

$$\left.\begin{array}{l}\text{(a) } (H_2O)_2 + (H_2O)_2 \rightleftharpoons (H_2O)_4 \\ \text{(b) } (H_2O)_3 + (H_2O) \rightleftharpoons (H_2O)_4\end{array}\right\} \text{tetramer}$$

$$\left.\begin{array}{l}(H_2O)_2 + (H_2O)_3 \rightleftharpoons (H_2O)_5 \\ (H_2O)_4 + (H_2O) \rightleftharpoons (H_2O)_5\end{array}\right\} \text{pentamer}$$

$$\left.\begin{array}{l}(H_2O)_2 + (H_2O)_4 \rightleftharpoons (H_2O)_6 \\ (H_2O)_3 + (H_2O)_3 \rightleftharpoons (H_2O)_6 \\ (H_2O)_5 + H_2O \rightleftharpoons (H_2O)_6\end{array}\right\} \text{hexamer} \quad (25)$$

If one assumes that complexes of a particular type, i.e., a tetrameter $(H_2O)_4$, are formed by only one of the reactions of (25), the reaction constants are given by

$$K_{assc}{}^a = C_t/C_2^2; \qquad K_{assc}{}^b = C_t/(C_1C_3) \quad (26)$$

where C_t is the total concentration of the product, which is proportional to $(H_2O)_3{}^+H$ peak intensity, and C_i is the concentration of the ith component of the reaction.

Let C_a and C_b be the concentrations in two partial reactions by which $(H_2O)_4$ is formed, then

$$C_c = C_a + C_b \quad (27)$$

and

$$(K_{assc}{}^a)' = C_a/C_2^2; \qquad (K_{assc}{}^b)' = C_b/(C_1C_3) \quad (28)$$

The ratio of the product concentrations of two partial reactions according to eq 28 is

$$\frac{C_a}{C_b} = \frac{C_2^2}{C_1C} \frac{(K_{assc}{}^a)'}{(K_{assc}{}^b)'} = CK \quad (29)$$

where

$$C = C_2^2/(C_1C_3); \qquad K = (K_{assc}{}^a)'/(K_{assc}{}^b)'$$

Substitution of (29) in (27) yields

$$C_a = C_t[CK/(1 + CK)]; \qquad C_b = C_t\,[1/(1 + CK)] \quad (30)$$

Then $(K_{assc}{}^a)'$ and $(K_{assc}{}^b)'$ will be represented as

$$(K_{assc}{}^a)' = \frac{C_t}{C_2^2} \frac{CK}{1 + CK}; \qquad (K_{assc}{}^b)' = \frac{C_t}{C_1C_2} \frac{1}{1 + CK}$$

TABLE III. Experimental Enthalpies of Water Clusters in a Vacuum (kcal/mol)

cluster	reaction pathway	$-\Delta H_{react}$	$-\Delta H_{tot}{}^{n}$	$-\Delta H_{mol}$
$(H_2O)_2$	1 + 1	4.2 ± 1.1	4.2	2.1
$(H_2O)_3$	2 + 1	6.7 ± 0.9	10.9	3.6
$(H_2O)_4$	2 + 2	32.0 ± 1.2	33.6	8.4
	3 + 1	15.8 ± 0.8		
$(H_2O)_5$	3 + 2	35.2 ± 0.7	46.9	9.4
	4 + 1	9.8 ± 1.2		
$(H_2O)_6$	3 + 3	32.1 ± 1.0		
	4 + 2	22.8 ± 1.1	55.0	9.2
	5 + 1	3.7 ± 1.3		

Taking the logarithm of these equations with regard to (26), one obtains

$$\ln (K_{assc}{}^{a})' = \ln K_{assc}{}^{a} - [\ln (1 + CK) - \ln (CK)] \quad (31a)$$

$$\ln (K_{assc}{}^{b})' = \ln K_{assc}{}^{b} - \ln (1 + CK) \quad (31b)$$

Since the reaction enthalpy is derived from K_{assc} values (see eq 10), eq 31a and 31b can be written

$$\Delta H_a' = \Delta H_a - \Delta H_a{}^{add} \quad (32a)$$

$$\Delta H_b' = \Delta H_b - \Delta H_b{}^{add} \quad (32b)$$

where $\Delta H_a{}^{add}$ and $\Delta H_b{}^{add}$ are additional terms. According to the Gess law

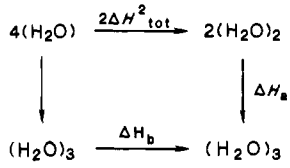

the total enthalpy of a tetramer formation can be calculated as a sum

$$\Delta H_{tot}{}^{4} = (2\Delta H_{tot}{}^{2} + \Delta H_{tot}{}^{3} + \Delta H_a + \Delta H_b)/2 \quad (33)$$

or, with regard to (32a) and (32b)

$$\Delta H_{tot}{}^{4} = (2\Delta H_{tot}{}^{2} + \Delta H_{tot}{}^{3} + \Delta H_a' + \Delta H_b')/2 + (\Delta H_a{}^{add} + \Delta H_b{}^{add})/2 \quad (34)$$

The correction term $(\Delta H_a{}^{add} + \Delta H_b{}^{add})/2$ can be estimated from a comparison of enthalpy values calculated by using eq 34 with those calculated theoretically.

In the same way total enthalpies of pentamer and hexamer formation were calculated (Table III).

2. Theoretical Calculations

In order to compare experimental results with theory we have calculated enthalpies of formation of small water clusters. Calculations were performed by using conventional methods of statistical physics and available data on potential energies of $(H_2O)_n$ cluster formation in a vacuum, on structure,[44] and on vibrational frequencies.[52]

An equilibrium ideal gaseous mixture was considered in which association and dissociation reactions can take place:

$$a(H_2O)_m + b(H_2O)_n \rightleftharpoons (H_2O)_{(am+bn)} \quad (35)$$

The enthalpy of one of these reactions can be obtained from K_{assc} values according to eq 10, while K_{assc} can be represented by sums taken over the states of molecules that participate in the reaction[48]

$$K_{assc} = P^{1-(a+b)} \frac{Q_{(am+bn)}}{(Q_m)^a (Q_n)^b} \exp\left(\frac{E_{dis}}{RT}\right) \quad (36)$$

where P is pressure, Q_i is the statistical sum for the ith complex, and E_{dis} is the dissociation energy of the complex equal to

$$E_{dis} = \Delta U_0 - \Delta E \quad (37)$$

ΔU_0 is the difference between zero-point vibrational energies of complexes and reagents; ΔE is the potential energies difference.

Thus, when eq 34 and 35 are taken into account, the reaction enthalpy is given by

$$\Delta H_{react} = \Delta H_{tr\text{-}rot} + \Delta H_{vibr} + \Delta E \quad (38)$$

where $\Delta H_{tr\text{-}rot}$ is the change of translational-rotational enthalpy and $\Delta H_{vibr} = \Delta E_{vibr}$.

The vibrational energy of the mth complex was calculated as

$$U_m{}^{t} = U_m{}^{0} + RT\sum \frac{x_i e^{-x_i}}{1 - e^{-x_i}} \quad (39)$$

where

$$U_m{}^{0} = (RT/2)\sum x_i \quad (40)$$

is the zero-point vibrational energy, while

$$x_i = h\nu_i/kT = \theta_i/T \quad (41)$$

where $\theta_i = 1.43888\nu_i$ (ν_i stated in cm) is the characteristic temperature of the ith complex. The form of eq 39–41 was chosen for the purpose of programming convenience. Vibrational frequencies were taken from ref 52. U_m and E_m are listed in Table IV. Calculated enthalpies for all possible association reactions, with the exception of that for a hexamer (in this case the reaction for monomers only was considered) are listed in Table V. The difference between ΔH_{react}, obtained with regard to external vibrations only and to the full frequency set comprises not more than 4% in the case of a dimer and decreases with an increase of n. Therefore it is quite reasonable to calculate enthalpies of water clusters by using a rigid body model, decreasing the computation time substantially and omitting additional calculations of intermolecular frequencies.

TABLE IV. Vibrational (U_m) and Potential (E_m) Energies of Water Clusters (kcal/mol)

	full set of frequencies		with regard to external vibrations		
cluster	$U_m{}^{0}$	$U_m{}^{T}$	$U_m{}^{0}$	$U_m{}^{T}$	$-E_m$
$(H_2O)_2$	27.4	29.6	1.8	4.0	6.1
$(H_2O)_3$	42.3	46.4	4.0	8.1	16.8
$(H_2O)_4$	58.2	63.7	7.4	12.8	37.9
$(H_2O)_5$	73.2	80.7	9.7	17.2	53.2
$(H_2O)_6$	87.9	97.6	11.7	21.4	64.6

3. Discussion

It has been shown above that the enthalpy $\Delta H_{tot}{}^{2} = -4.2$ kcal/mol of an H_2O dimer formation is relatively low, the value being in good agreement with that of $\Delta H = -5.1$ kcal/mol measured by IR spectroscopy,[53] which indicates that water molecule association at the emitter occurs under equilibrium conditions, similar to the case

TABLE V. Calculated Enthalpies of Water Clusters at 300 K (kcal/mol)

cluster	reaction pathway	$-\Delta H_{tr\text{-}rot}$	ΔH_{vibr}	$-\Delta E$	$-\Delta H_{react}$	ΔH_{totl}^n
$(H_2O)_2$	1 + 1	2.4	3.8	6.1	4.7	4.7
$(H_2O)_3$	1 + 1 + 1	4.8	7.7	16.8	13.9	13.9
	2 + 1	2.4	3.9	10.7	9.2	
$(H_2O)_4$	1 + 1 + 1 + 1	7.2	12.1	37.9	33.0	
	2 + 1 + 1	4.8	8.3	31.8	28.3	33.0
	2 + 2	2.4	4.5	25.7	23.6	
	3 + 1	2.4	4.4	21.1	19.1	
$(H_2O)_5$	1 + 1 + 1 + 1 + 1	9.6	16.2	53.2	46.6	
	2 + 1 + 1 + 1	7.2	12.4	47.1	41.9	
	2 + 2 + 1	4.8	8.6	41.0	37.2	46.6
	4 + 1	2.4	4.1	15.3	13.6	
	3 + 2	2.4	4.7	30.3	28.0	
	3 + 1 + 1	4.8	8.5	36.4	32.7	
$(H_2O)_6$	1 + 1 + 1 + 1 + 1 + 1	11.9	20.2	64.6	56.3	56.3

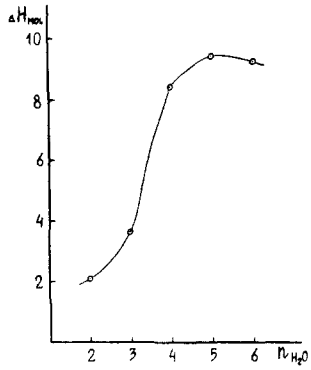

Figure 10. Variation of the enthalpy ΔH_{mol} per water molecule with the number of water molecules in a cluster n_{H_2O}.

of base molecules. Attachment of the next water molecule, i.e., formation of a dimer, occurs with a much greater energy gain (−6.7 kcal/mol), which results in an increase of the mean enthalpy value per water molecule $\Delta H_{mol} = \Delta H_{tot}/n$ by a factor of 1.7 for a trimer as compared to a dimer. For a tetramer the ΔH_{tot}^4 increase is still more noticeable: $\Delta H_{tot}^4 - \Delta H_{tot}^3 = -22.7$ kcal/mol, ΔH_{mol} being 2.3 times greater. However, for still higher water polymers $(H_2O)_5$ and $(H_2O)_6$ increments of ΔH_{tot}^n decrease gradually, ΔH_{mol} values being approximately constant (Figure 10). ΔH_{mol} change must be accounted for by the structure peculiarities of small water clusters. An appreciable increase of ΔH_{tot}^n values for $n \geq 3$ is probably due to formation of cyclic configurations in which every water molecule participates in two hydrogen bonds, being both a proton donor and a proton acceptor. The peculiarities of the ΔH_{mol} vs. n_{H_2O} plot must therefore reflect the strain of hydrogen bonds in the complexes.

It is interesting to note that ΔH_{mol} values for complexes with $n = 5$ and 6 are close to that of the boiling heat of liquid water (−9.7 kcal/mol).

In the following discussion we shall consider theoretical results for similar clusters (Table VI). Most of the calculations have been done by using the so-called Hartree–Fock approximation, since it is still impossible at present to do precise ab initio computation of systems that contain more than 15 atoms.[48] Quantitative results of these works, which depend, on one hand, on dimensions of the chosen basis and, on the other hand, on the correlation correction, differ noticeably. Lately, a great deal of calculations have been done by using semiempirical intermolecular potentials in the conjugate

TABLE VI. Enthalpies ΔH and Energies E_m of Water Cluster Formation (kcal/mol)

	$-\Delta H$					
	present investigation			$-E_m$		
cluster	expt	theor	[47][a]	[47]	[45]	[44]
$(H_2O)_2$	4.2	4.7	3.28	5.44	4.4	6.1
$(H_2O)_3$	10.9	13.9	10.37	14.81	12.3	16.8
$(H_2O)_4$	33.6	33.0	18.49[b]	25.11[b]	20.54	37.9
$(H_2O)_5$	46.9	46.6	26.24[c]	35.5[c]	26.0	53.1
$(H_2O)_6$	55.0	56.3			31.8	64.5

[a] Calculations for 400 K. [b] Tetrahedral structure. [c] Cage-like structure.

additivity approximation, the results being in good agreement with the experiment.

Below we shall consider a few works that give, from our point of view, the most reliable data on energies and configurations of water clusters with the number of H_2O molecules about the same as the experimental one. Ab initio computations by the LCAO SCF method[44] predicted a value of $E = -6.09$ kcal/mol for an equilibrium linear dimer geometry. It has been also shown that hydrogen bonding causes a noticeable electron density redistribution over the interacting water molecules: hydrogen atoms belonging to acceptor molecules become more positively charged, which makes them preferable potential donors in subsequent interactions, while hydrogen atoms belonging to donor molecules acquire additional negative charges and thus become stronger proton acceptors. This facilitates cyclization of three water molecules with the formation of a planar structure with much smaller energy than that for a linear geometry:[44] $E_{cycl}^3 - E_{lin}^3 = -2.2$ kcal/mol. In the case of a tetramer this difference equals −13.4 kcal/mol.[44] These effects result from the cooperativity of interactions in complexes, which is proved by consideration of other possible schemes of hydrogen bonding. For example, in the case of a tetramer $(H_2O)_4$ that has the D_{2h} symmetry (opposite molecules being donors or acceptors) the stabilization energy decreases to −17.2 kcal/mol. The same is true for a hexamer, since in this case cooperativity of OH···OH···OH chains characteristic of C_n structures is lacking. At the same time transformation of a C_n structure to a S_n one, which occurs when alternating water molecules are reflected in the plane of oxygen atoms, results in an additional stabilization energy.[44] Agreement between experimental enthalpy values and those calculated by us using E_m energies for C_n structures (Table VI) suggests that water complexes attain planar C_n configurations.

A great number of possible dimer, trimer, tetramer, pentamer, hexamer, hectamer, and octamer configurations were considered[45] by using an analytical form of the Hartree–Fock potential (AFHF) with the aim of elucidating minimum-energy configurations. Theoretical results for dimers and trimers agree quantitatively both with the experimental results and with other quantum mechanical computations (Table VI), the preferable dimer configuration being linear while that of a dimer and tetramer is cyclic. The interaction between two molecules in a gaseous phase at $T = 298$ K was also considered in ref 45. A dimerization enthalpy of −4.6 kcal/mol for an open configuration was obtained with regard to a correlation correction which coincides with the experimental value. Calculated energies for

higher polymers were noticeably smaller as compared to the experimental values, but the general tendency of the E_{mol} vs. n_{H_2O} plot agreed qualitatively with the experiment.

The structure of water polymers with $n \geq 4$ is not unique,[45] energies for different complex configurations being close to each other. Nearly the same conclusions can be drawn from the investigation of energetics and thermodynamics of small water clusters (n = 2–5) using the EPEN potential,[47] the only predicted structures for $(H_2O)_2$ and $(H_2O)_3$ complexes being linear trans and cyclic configurations, respectively. In the case of a tetramer and a pentamer there exists a great number of local energy minima, the deepest of which correspond to closed structures: a pyramid tetramer and a cage-like pentamer.[47] Calculated dimer and trimer enthalpies were close to the experimental ones, while for higher polymers those values differed drastically. Thus, it can be concluded that water dimers exist in a linear form and trimers in a cyclic form. The most probable structures of water complexes with $n > 3$, revealed by FIMS in a vacuum, are presumably planar cyclic structures formed at the emitter surface. This suggestion is substantiated by recent calculations by Poltev et al.,[49] who used atom–atom potential functions with refined parameters, which were chosen by comparison with the thermodynamics of ice. It was shown[48] that global energy minima for $(H_2O)_n$ (n = 3–6) complexes correspond to almost planar polyhedrons (with the exception of a hexamer $(H_2O)_6$), oxygen atoms being situated in the vertices and stabilizing the structure by OH···O hydrogen bonds. Only a trimer $(H_2O)_3$ with strained bonds shows deviations from linearity of about 20°.

The conclusion about the cyclic structure of water complexes can be also drawn from observations on their deviation by electric field.[54] It has been shown that the degree of refocusing of polar H_2O monomers was very high, the same being true for dimers with relatively high dipole moments. However, for higher complexes—$(H_2O)_3$, $(H_2O)_4$, $(H_2O)_5$, and $(H_2O)_6$—refocusing was very weak, which is attributed to the existence of cyclic structures with nearly zero total dipole moments.

The results presented above show that the TD-FIMS method, developed by us, provides valuable information about enthalpies of equilibrium association of water molecules in a vacuum. Analysis of the experimental data and their detailed comparison with theory lead to a conclusion about the formation of planar cyclic water complexes at the emitter surface.

Energetical preference of cyclic structures may appear to be significant in the interaction between water molecules and biomolecules, in particular, with nucleic acid bases, which possess different nucleophilic atom groups.

B. Enthalpies of Mono-, Di-, and Trihydrates of Nucleic Acid Bases

Hydration of bases was achieved when water and bases were supplied simultaneously to the emitter from two evaporators (Figure 4). Under certain conditions of evaporation a zone of high molecular density was formed near the emitter surface, where base collisions with H_2O molecules occurred, thus leading to formation of hydrated complexes. Experiments with pyrimidine bases are described first.[55,56]

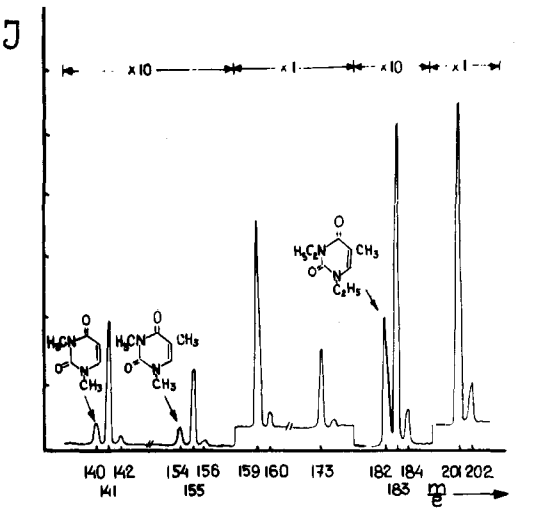

Figure 11. FI mass spectrum of the mixture 1,3MeUra + 1,3MeThy + 1,3EtThy + H_2O, registered with a tungsten emitter.

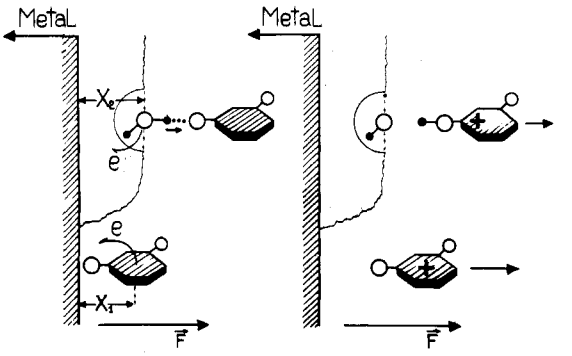

Figure 12. Mechanism of the $(MH)^+$ ion creation during ionization of a dimer $M{\cdot}H_2O$ in electric field F. x_1 and x_2 are ionization distances.

1. Uracil Methyl Derivatives

Alkyl derivatives of uracil were used, which were synthesized by conventional procedures and purified by repeated recrystallization from water at the Institute of Biochemistry and Biophysics (Polish Academy of Sciences). A typical FI mass spectrum of hydrated 1,3MeUra is shown in Figure 11, together with the spectra of 1,3MeThy and 1,3EtThy registered under similar conditions. These spectra show molecular ions of the bases M^+ at m/e 140, 154, and 182 and also $[MH(H_2O)_n]^+$ (n = 0, 1) ions produced by base mono- and dihydrates: $M{\cdot}H_2O$ and $M(H_2O)_2$. Protonated ions $(MH)^+$ and $(MH{\cdot}H_2O)^+$ appear instead of the expected $(M{\cdot}H_2O)^+$ and $[M(H_2O)_2]^+$ ions due to the mechanism of field ionization of hydrated complexes, which involves proton transfer similar to the case of water self-associates. Figure 12 illustrates details of the process. When base and water molecules collide, a hydrogen-bonded complex $M{\cdot}H_2O$ is formed on the emitter surface with the lifetime τ_i and is then ionized by tunneling of an oxygen electron into the metal electrode. This results in weakening of the O–H bond, which, in turn, causes an increased probability of an electron jump to an electrophylic base atom to which the water molecule is bound:

$$M + H_2O \rightleftharpoons M{\cdot}H_2O \xrightarrow{\text{ionization}} (M{\cdot}H)^+ + OH + e^- \text{ (into the metal)} \quad (42)$$

TABLE VII. Enthalpies of Mono-, Di-, and Trihydrates of Nucleic Acid Bases in a Vacuum (kcal/mol)

base	$M{\cdot}H_2O$		$(M{\cdot}H_2O){\cdot}H_2O$		$(M(H_2O))_2{\cdot}H_2O$
1MeUra	11.2	7.6[a]	9.0	8.7[a]	
1,3MeUra	12.9	7.6[a]	10.8	8.7[a]	6.2
1MeThy	10.4	7.6[a]	9.5	8.7[a]	
1,3MeThy	8.7	6.9[a]	10.2	6.5[a]	
1,3EtThy	10.8		10.3		
1MeCyt	11.4	12.6[a]	8.6	10.6[a]	
4MeCyt	10.7		10.5		
5MeCyt	11.6		10.3		
1,4MeCyt	12.1	12.8[a]	9.0	7.4[a]	
4,4MeCyt	10.4		8.5		
1,4,4MeCyt	11.8	12.9[a]	7.0	7.4[a]	
7MeAde	11.1	12.8[a]		8.7[a]	
9MeAde	10.6	9.9[a]	7.75	8.5[a]	7.2
6,6MeAde	10.1	9.0[a]		11.0[a]	
6,6,9MeAde	8.3	7.8[a]	6.7	7.8[a]	5.9
6,9MeAde	9.2	9.9[a]	7.05	8.0[a]	6.0
2,2,9MeGua	14.1		8.4		

[a] Theoretical results.[35]

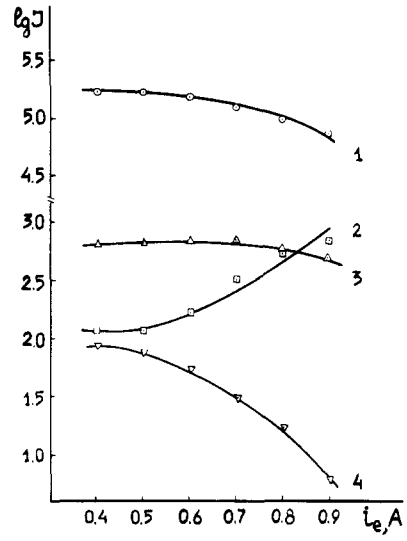

Figure 13. Variation of the ionic currents with temperature: (1) H_3O^+; (2) M^+; (3) $(MH)^+$; (4) $(MH{\cdot}H_2O)^+$. M = 1,3MeUra.

It should be noted that it is water molecules and not bases which are ionized, since ionization potentials of molecules in the complex differ significantly and the distance x_1 at which ionization of bases takes place also differs from the corresponding value x_2 for H_2O. x_2 characterizes presumably the thickness of condensed water film, since ions can be detached only from its surface layers. Observation of the MH^+ ions is indicative of a specific cluster structure of the water film (Figure 12) on the tungsten surface. When a platinum emitter was used instead of the tungsten one with the same experimental conditions, mass spectra were changed noticeably.[55]

Low peak intensity for the $(M{\cdot}H_2O)^+$ ion (m/e 158) (not for the $(MH)^+$ ion as in the case of the tungsten emitter) suggests that the association occurs preferentially in the gaseous phase. In this case the $(M{\cdot}H_2O)^+$ ion is formed by detachment of a π-electron from a base molecule without a proton transfer.

The $(MH{\cdot}H_2O)^+$ ions at m/e 159, 173, and 201 were formed by the same mechanism as the $(MH)^+$ ions (Figure 12).

The analysis of the ionic current I_{MH} and $I_{(MH{\cdot}H_2O)^+}$ dependences on water concentration ($I_{H_2O^+}$, $I_{H_3O^+}$) in the reaction zone at the emitter has shown that both mono- and dihydrates of bases were formed by the first-order reaction with respect to water. This implies that hydration occurs via consecutive binding of single H_2O molecules:

$$M + H_2O \rightleftharpoons M{\cdot}H_2O + H_2O \rightleftharpoons M(H_2O)_2 + \ldots \quad (43)$$

The mass spectra enable us to obtain readily apparent association constants K_{assc} for the hydrates, e.g., for $M{\cdot}H_2O$

$$K_{assc}^{M{\cdot}H_2O} = I_{MH^+}/(I_{M^+}I_{H_3O^+}) \quad (44)$$

The calculations were done by using (similar to the case of water self-association), instead of a weak ionic current $I_{H_2O^+}$, a much greater current $I_{H_3O^+}$, which is proportional to $I_{H_2O^+}$. The value of $K_{assc}^{M(H_2O)_2}$ for the binding of the second water molecule to the $M{\cdot}H_2O$ complex was calculated similarly, $(MH{\cdot}H_2O)^+$, $(MH)^+$, and $(H_3O)^+$ ion intensities being used.

On the basis of $K_{assc}^{M{\cdot}H_2O}$ and $K_{assc}^{M(H_2O)_2}$ values which were obtained from the experimental plots lg I vs. i_e (Figure 13) van't Hoff enthalpies of 1,3 MeUra mono- and dihydrates in a vacuum were derived. Similar dependences were plotted for other uracil methyl derivatives, and enthalpies were calculated in the same manner (Table VII).

2. Cytosine Methyl Derivatives

Mono-, di-, and trimethyl derivatives of cytosine were used, which were synthesized at the Department of Organic Chemistry, Kharkov State University. FI mass spectra of hydrated N-methylated cytosines are in complete qualitative agreement with those of alkyluracils.

FI mass spectra of mechanical mixtures 1,4,4 MeCyt + 1,4MeCyt + H_2O; 5MeCyt + H_2O; 1MeCyt + H_2O; and 7MeCyt + H_2O were recorded in the temperature range 295–320 K. lg I vs. i_e plots were used to obtain lg K_{assc} vs. T_e plots for each of the hydrates, from which the enthalpies of hydration reactions were calculated (Table VII).

To reveal possible electric field effect on the measured enthalpy (ΔH_{hydr}) values, a detailed study of temperature dependences of K_{assc} for 1,4,4 MeCyt and 1,3 MeUra mono- and dihydrates was undertaken at three different emitter potentials: 3, 4, and 5 kV; the results of this study are listed in Table VIII.

Comparison of these data with the mean value ΔH_{hydr} taken over several measurements (Table VIII) shows that deviations of the measured values lie within the

TABLE VIII. Hydration Enthalpies (kcal/mol) of 1,4,4MeCyt and 1,3MeUra Obtained for Different Emitter Potentials U_e(kV)

	$M{\cdot}H_2O$			$M{\cdot}(H_2O)_2$				
base	$U_e = 3$	$U_e = 4$	$U_e = 5$	$U_e = 3$	$U_e = 4$	$U_e = 5$	$M{\cdot}H_2O$	$M{\cdot}(H_2O)_2$
1,3MeUra	12.4	12.2	12.6	10.2	10.5	10.4	12.9 ± 1.4	10.8 ± 0.8
1,4,4MeCyt	12.0	11.7	11.8	7.2	6.7	7.3	11.8 ± 0.9	7.0 ± 1.3

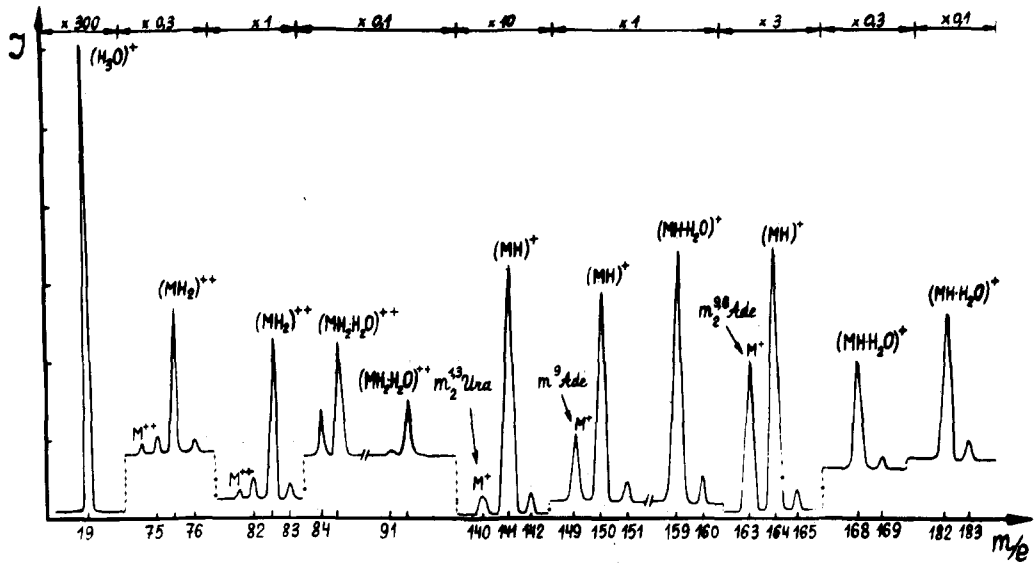

Figure 14. FI mass spectrum of the mixture 9MeAde + 6,6MeAde + 1,3MeUra + H_2O, registered with a tungsten emitter.

experimental error, thus indicating that electric field effect on the experimental ΔH_{hydr} values can be neglected.

3. Adenine Methyl Derivatives

Hydration of *N*-methyladenines, which were synthesized and purified at the Institute of Biochemistry and Biophysics, Polish Academy of Sciences (Poland), was studied[58] by using three-component mechanical mixtures of *N*-methyladenines, which were placed together with 1,3MeUra into one of the evaporators. 1,3MeUra was used as "an external temperature indicator" since its hydration (as well as that of methylcytosines) was studied earlier at different temperatures measured by a thermocouple.

For subsequent experiments two different methyladenines were chosen so that one of the bases was a component of the previous pair and thus served as "a secondary temperature indicator", provided that mass numbers of the mixture components and possible hydrated complexes did not coincide.

Mass spectrum of a ternary system—9MeAde + 6,9MeAde + 1,3MeUra—in the presence of water vapor (Figure 14) shows two intense peaks at m/e 150 and 164 for protonated ions $(MH)^+$, which were produced by ionization of neutral $M{\cdot}H_2O$ hydrates followed by a proton transfer (Figure 12). The mass spectrum shows also peaks at m/e 168 and 182 for $(MH{\cdot}H_2O)^+$ ions, which resulted from ionization of dihydrate $M(H_2O)_2$. Concentrational dependences lg $I_{MH^+} = f(I_{H_3O^+})$ and lg $I_{MH{\cdot}H_2O} = f(I_{H_3O^+})$ for *N*-methyladenines, similar to the case of alkyluracils and methylcytosines, reflect the first-order reactions with respect to water, which in turn indicates a stepwise character of hydration reactions.[43]

The mass spectrum of the mixture under consideration (Figure 14) in the presence of water molecules shows also a set of peaks corresponding to doubly charged ions M^{2+}, $(MH)^{2+}$, and $(MH{\cdot}H_2O)^{2+}$, in contrast to the case of alkyluracils and methylcytosines studied under the same experimental conditions. The doubly charged ions appear due to the comparatively low ionization potentials of adenine as compared to that of diketopyrimidines.[59,60] The difference in ionization potential, concerning the highest occupied electron orbital, between these two groups of bases is also reflected in their protonation behavior in aqueous solutions.[61]

Doubly charged ions are produced, obviously, by successive ionization of hydrated clusters $M(H_2O)_n$ (n = 1–3) according to the following scheme:

$$M{\cdot}H_2O + H_2O \rightleftharpoons M(H_2O) \xrightarrow{\text{ionization } (-e^-)}$$

$$(MH{\cdot}H_2O)^+ + OH \xrightarrow{\text{ionization } (-e^-)} (MH_2)^{2+} + OH \quad (45)$$

The $(MH{\cdot}H_2O)^{2+}$ ions were generated from triple $M(H_2O)_3$ hydrates by a similar mechanism.

The hydrate mass spectra of binary mixtures 6,9MeAde + 6,6,9MeAde, 7MeAde + 6,6,9MeAde, and 6,6MeAde + 6,6,9MeAde qualitatively resemble the mass spectrum described above.

Apparent association constants $K_{assc}^{M{\cdot}H_2O}$ and $K_{assc}^{M(H_2O)_2}$ were calculated by using peak intensities for the ions MH^+, M^+, and H_3O^+ and $(MH{\cdot}H_2O)^+$, $(MH_2)^{2+}$, $(MH)^+$, and H_3O^+, respectively.

Hydration enthalpies ΔH_{hydr} for $M{\cdot}H_2O$ complexes which were derived from the slope of van't Hoff plots are listed in Table VII.

In the case of doubly charged ions $(MH_2)^{2+}$ lg I vs. i_e and van't Hoff plots for association constants K_{assc} are similar to those of singly charged ions, which can be readily seen for MH_2^{2+} (m/e 82.5) and $(MH{\cdot}H_2O)^+$ ions of 6,9MeAde, originating from the same common parent hydrate $M(H_2O)_2$.[58] For both ions lg I vs. i_e and lg K_{assc} vs. T_e plots take the same form and hydration enthalpies derived from the slopes proved to be the same within experimental error.[58] The value of ΔH_{hydr} = −7.6 kcal/mol in Table VII for the reaction 6,9 MeAde·H_2O + H_2O ⇌ 6,9MeAde·$(H_2O)_2$ is the average value of the two enthalpies.

In order to reveal possible electric field effect on ΔH_{hydr} values, in the case of *N*-methyladenines lg I dependence on i_e was investigated at different emitter potentials U_e. Electric field F was found to have no effect on the measured enthalpy values.

4. Guanine Methyl Derivatives

The FI mass spectrum of trimethylguanine 2,2,9MeGua registered at the emitter temperature 303

K was similar to those of *N*-methyladenines (Figure 14). Besides the most commonly observed ions MH^+ and $(MH{\cdot}H_2O)^+$, the spectrum shows also doubly charged ions M^{2+}, MH^{2+}, and MH_2^{2+}, produced by the above-considered mechanism. However, unlike the case of *N*-methyladenines, with the same conditions of supplying the substance to the reaction zone, $(MH_2{\cdot}H_2O)^{2+}$ ions for the triple $M(H_2O)_3$ hydrates were not observed. This suggests that the third water molecule binding to a double $M{\cdot}(H_2O)_2$ hydrate in the case of 2,2,9MeGua results in a smaller energy gain as compared to the case of *N*-methyladenines.

Enthalpies of 2,2,9MeGua mono- and dihydrates, derived from association constant K_{assc} temperature dependences, are listed in Table VII.

5. Discussion

Alkyluracils. For all investigated compounds enthalpies of mono- and dihydration exceed noticeably those of $(H_2O)_2$ and $(H_2O)_3$ cluster formation, which are equal to −4.2 and −6.7 kcal/mol, respectively (Table III). Small changes of hydration enthalpies $\Delta H_{hydr}^{M{\cdot}H_2O}$ and $\Delta H_{hydr}^{M(H_2O)_2}$ observed for dimethyluracils (1,3MeUra and 1,3MeThy) as compared to monomethyl derivatives (1MeUra and 1MeThy) indicate that the contribution of C=O groups to the hydration energy is greater than that of the N(3)–H group. This, in turn, leads to a conclusion that Ura and Thy molecules have two strong binding sites for water molecules located near the O(2) and O(4) atoms.

This conclusion contradicts theoretical predictions,[38] according to which both water molecules are located near the same C(4)=O group in the case of 1,3MeUra. However, other theoretical calculations[28-31] show that two main minima located in the vicinity of the C(2)=O and C(4)=O groups exist for the "base–H_2O" system. It must be these sites that participate in the strongest binding between a base and two H_2O molecules. Formation of binding configurations of the O(2)...H_2O...H_2O...N(3) type appears to be less favorable since it has been shown experimentally that the substitution of the C_2H_5 group for the N(3) proton has almost no effect on the energy of the (Thy + $2H_2O$) complex formation (Table VII). It should be noted that the third water molecule binding to a dihydrate of 1,3MeUra is accompanied by a noticeably smaller energy gain (Table VII). Thus, it can be concluded that each Ura or Thy molecule has two strong binding sites for water molecules located near the C=O groups.

Methylcytosines. From the values of enthalpies for the reactions $M + H_2O \rightleftharpoons M{\cdot}H_2O$ for all methylcytosines studied (Table VII), it follows that a water molecule interacts most favorably with the N(3),CO groups of cytosine, the interaction energy ranging from −10.4 to −12.1 kcal/mol. Besides, two other strong binding sites exist, namely, polar atom groups N(4)–H,N(3) and N(1)–H,CO.

Thus, it can be concluded that cytosine, unlike uracil, has three strong binding sites for water located in the polar part of the molecule. This conclusion is in accordance with the results of quantum mechanical and atom–atom computations of cytosine monohydration[28-31,49,63] as well as of methylcytosine mono- and dihydration.[38] It should be noted that, unlike uracil methyl derivatives, in the case of cytosine derivatives experimental and theoretical[38] enthalpies for both types of reactions agree quantitatively (Table VII).

Methyladenines. Monomethylated adenines exhibit more favorable properties as compared to dimethyl derivatives and 6,6,9MeAde, methylation influencing substantially both monohydration (contrary to the case of pyrimidine bases) and, to a smaller extent, dihydration reaction (Table VII). Consecutive water binding by any of the adenine monohydrates is energetically less favorable, while the third molecule is bound by dihydrates with approximately the same enthalpy as the second molecule bound by monohydrates.

Theoretical schemes of adenine hydration[28-30,34,48,63] give the same qualitative predictions: the existence of three deep minima with slightly differing energies located in the plane of the purine ring between the two ring nitrogens, N(3) and N(9), and also between either of the two other ring nitrogens, N(7) and N(1), and the exocyclic amino group NH_2. It is obvious then that single methylation at N(7) or N(3) leaves the two strong binding sites unperturbed. Therefore, as expected, both bases exhibit the same monohydration properties. The increase of the 7MeAde hydration enthalpy as compared to that of 9MeAde is confirmed theoretically[62] and can be accounted for by a greater binding energy of the water molecule at N(3) and N(9) sites of 7MeAde.

In the case of adenine dimethyl derivatives only one strong binding site is left: N(7), N(amino) in the case of 6,9MeAde (of the two possible rotational isomers, the one with the aminomethyl group trans with respect to imidazole N(7) is presumably more stable thermodynamically). A weaker binding site is also found at N(3) and N(9) in the case of 6,6MeAde. The inverse order of the enthalpies for these two hydrates as compared to the theoretical one (Table VII) necessitates further studies.

Finally, in the case of the fully N-methylated derivative 6,6,9MeAde all three hydrophilic sites are not sterically accessible, which has a marked effect on the enthalpy of monohydration.

Quantitative agreement between experimental and theoretical energies of the first and the second water molecules binding to *N*-methyladenines should be pointed out. According to the theory, binding of the second water molecule by monohydrates, except for 6,6MeAde, does not perturb the configuration and the binding energy of the first water molecule. Substantial gain in the dihydration enthalpy in the case of 6,6MeAde[62] results from direct additional interaction between the two water molecules located near the N(3) and N(9) atoms. We failed to verify this interesting prediction experimentally owing to low 6,6MeAde molecular concentration in the reaction zone.

2,2,9-Trimethylguanine. 2,2,9MeGua exhibits the greatest monohydration enthalpy among all purine and pyrimidine bases studied (Table VII). The enthalpy of the second water molecule binding to 2,2,9MeGua monohydrate is about 5.7 kcal/mol greater than the monohydration enthalpy. This result indicates that the guanine molecule, in contrast to other bases, possesses a specific hydration site that binds water molecules with much greater enthalpies than all the other polar groups of Gua. This site may be located between the C=O group and the N(7);[29,30,49,63] at the same time, according to recent ab initio computations by Del Bene,[34] the most

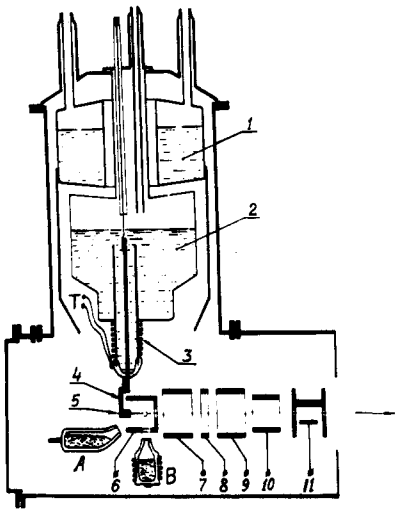

Figure 15. Low-temperature FI ion source: (1, 2) nitrogen and helium reservoirs; (3) heater; (4) emitter holder; (5) emitter; (6) counter electrode; (7–11) focusing lenses and the output slit unit; (A and B) glass evaporators.

stable configuration of Gua monohydrate with the energy E = −10.7 kcal/mol corresponds to binding of a water molecule at O(6)–N(1)H.

However, since most of the theoretical data on Gua monohydration[29,30,49,63] are in better quantitative agreement with the experiment (Table VII), it can be concluded that the most probable binding sites of water molecules in 2,2,9Gua mono- and dihydrates are O(6)–N(7) and N(1)–O(6), respectively.

C. Water Clusters and Polyhydrates of Bases at Low Temperatures

Observation of $M(H_2O)_n$, $n > 3$, complexes at T_e = 298 K is impeded by low density of the interacting particles near the emitter. At the same time studies on binding of the subsequent water molecules are of great interest in connection with the problem of contribution of different interactions (hydrophilic, hydrophobic) between water and base molecules to the total hydration energy.

Observation of large clusters becomes possible with a low-temperature modification of the ion source.[40] Therefore a FI ion source in which the emitter can be cooled to low temperatures has been designed.

1. Low-Temperature FI Ion Source

The low-temperature source (Figure 15) was designed on the basis of a gas ion source of the MI-1201 mass spectrometer and a helium cryostat (1).[64] The flange of the cryostat (2) was replaced by a low-temperature inlet with a glass insulator in which a high-voltage electrode cooled by liquid nitrogen was sealed. A copper holder (4) of a tungsten tip (5) is attached to the electrode. A counter electrode (6) and focusing lenses (7, 8) are installed on the low-temperature inlet with the aid of ceramic insulators. Lenses (9, 10) which belong to a deflector system (11) are installed on ceramic holders of the gas ion source. There is an emitter heating coil (3) on the low-temperature inlet. Temperature control was performed by a copper–constantan thermocouple (T). Compounds under investigation were supplied to the emitter from two evaporators (A, B).

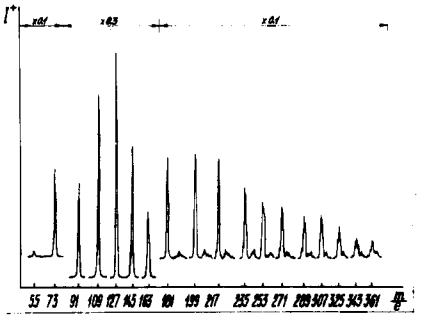

Figure 16. FI mass spectrum of water at 170 K.

2. Water Clusters

The FI spectrum[65] of water molecules condensed on the tungsten emitter (Figure 16) shows a set of cluster ions $(H_2O)_{n-1}H$ (n = 5, 6, ..., 20) that were produced by ionization of the corresponding neutral clusters $(H_2O)_n$. Unlike the water mass spectrum at 300 K with the most intensive peak at m/e 19, the low-temperature mass spectrum shows the most intensive peaks at m/e 127, 199, and 200 for water clusters with n = 8, 12, and 18 (Figure 16). At 170 K the clusters with eight water molecules are most stable. Increase of the emitter temperature is followed by a concentrational redistribution of the clusters in the condensed layer; the relative abundance of those with n = 7, 6, and 5 increases, while that of high clusters decreases, the maximum shifting to a water hexamer and then at 205 K to a trimer $(H_2O)_3$. At 285 K the most stable clusters are those with n = 3.

3. Uracil Methyl Derivatives

When base and water molecules are condensed simultaneously on the tungsten emitter surface, two types of complexes are formed: water clusters and base hydrates. At the same time the particles (original molecules and complexes) are ionized.

Figure 17 shows typical hydrate mass spectra of uracil methyl derivatives, registered at 170 K.[66] Unlike the case at 298 K, they show subsequent hydrate ions $MH\cdot(H_2O)_{n-1}^+$ and $M\cdot(H_2O)_n$ (n = 1–8) and ions $2M\cdot(H_2O)_m$ (m = 0–3) too. Two ion types, $MH(H_2O)_{n-1}^+$ and $M(H_2O)_n^+$, arise due to ionization of the same neutral complexes $M(H_2O)_n$ by two mechanisms. Protonated ions $MH(H_2O)_{n-1}^+$ were produced by ionization of a water molecule in the complex, followed by proton transfer either on a base or on the water molecule bound to the base. $M(H_2O)_n^+$ ions resulted from tunneling of an outer π-electron from the hydrated base molecule into the metal, the process not being followed by a proton transfer.

From the results presented above (see section IV) it may be inferred that enthalpies of mono- and dihydration ($\Delta H_{hydr}^{M\cdot(H_2O)_2}$ and $\Delta H_{hydr}^{M\cdot(H_2O)_2}$), derived from the association constant K_{assc} temperature dependences and from the ratio of corresponding ionic currents I_{MH^+}/I_{M^+} (in the case of monohydrates), are proportional to each other. This enables us to analyze qualitatively energies of hydration at low temperatures by studying the dependence of ionic currents, produced by hydrate ions $MH(H_2O)_{n-1}^+$, on the number of water

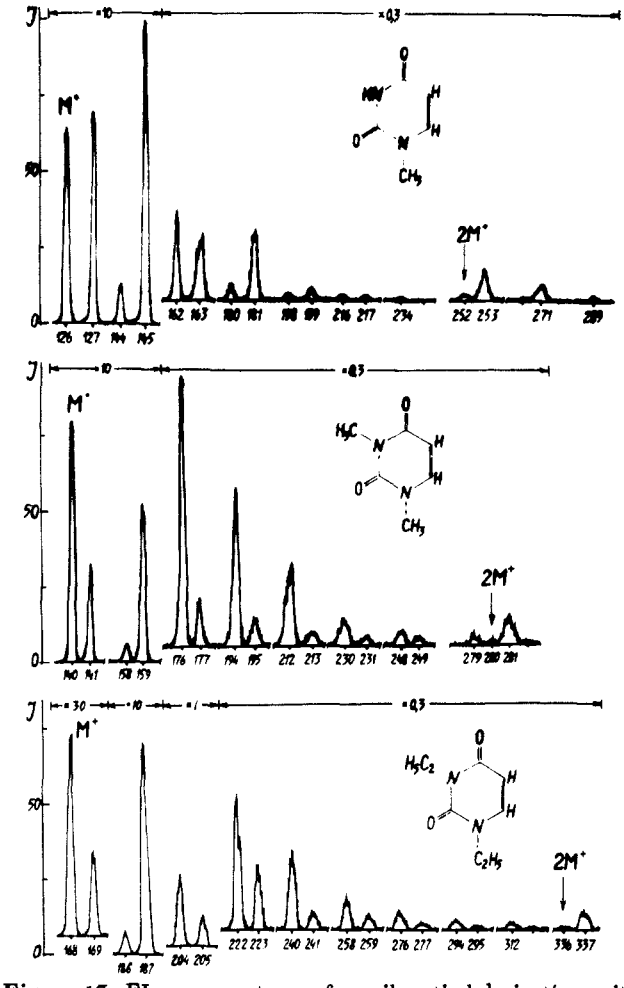

Figure 17. FI mass spectrum of uracil methyl derivatives with water molecules at T_e = 77 K.

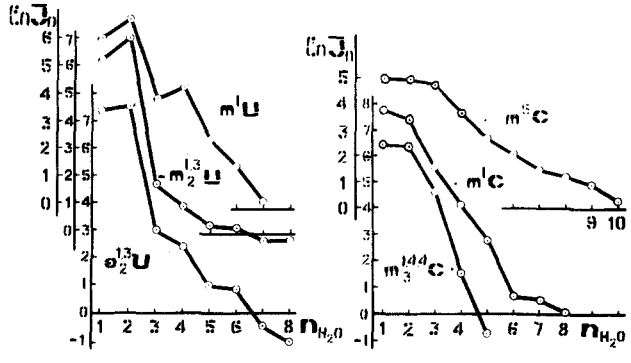

Figure 18. Variation of hydrate ion $MH\cdot(H_2O)_{n-1}$ intensities with the number of water molecules (n) in a cluster for Ura and Cyt.

molecules n in the complex.

For a number of methylated uracils the MH^+ and $(MH\cdot H_2O)^+$ peak intensities (Figure 18) show that enthalpy values of mono- and dihydration are close to each other ranging from −9 to −12.9 kcal/mol (Table VII). A drastic decrease of $MH(H_2O)_2^+$ ions which originate from the trihydrate $M(H_2O)_3$ is due to a noticeable decrease in the enthalpy of the third water molecule binding by the dihydrate $M(H_2O)_2$ as compared to enthalpies $\Delta H_{hydr}^{M\cdot H_2O}$ and $\Delta H_{hydr}^{M\cdot(H_2O)_2}$, which also agrees with the corresponding value of ΔH_{hydr} derived from the temperature dependence of K_{assc} (Table VII). Binding of subsequent water molecules does not result in such a substantial enthalpy decrease (Figure 18), the only exception being the $MH(H_2O)_3^+$ ion in the case of 1MeUra, which shows a substantial intensity increase probably caused by formation of an energetically more favorable structure as compared to the $M(H_2O)_3$ complex. A tetrahydrate $M(H_2O)_4$ of 1MeUra may have a cyclic structure formed by four water molecules and two polar uracil C=O groups, or it may exist as a distorted tetrahedron, which was predicted theoretically for the complex $Ura\cdot 4H_2O$.[37]

4. Cytosine Methyl Derivatives

Methylcytosines[66] show ln I_n dependences on the number of water molecules in a cluster (Figure 18) which are quite unlike those for methyluracils and suggest the existence of three strong binding sites on 5MeCyt and two sites on each of 1MeCyt and 1,4,4MeCyt molecules. This in turn suggests that methylation at the N(amino) in Cyt influences negligibly its mono- and dihydration behavior (Figure 18, curves 1 and 2). In the case of 5MeCyt subsequent water molecules (n = 4, 5, ...) are probably bound with greater energies as compared to both 1MeCyt and 1,4,4Cyt (Figure 18). It should be pointed out that while methylation of cytosine at N(1) has a marked effect on the nearest-neighbor water molecules, subsequent methylation, obviously, has a very small effect, at least as far as clusters of five water molecules are concerned.

Thus the results described above demonstrate the utility of the low-temperature FIMS method in the study of biomolecule hydration in a vacuum. Besides, the presence of the peaks at m/e 253, 271, and 289 for ions of 1MeUra·1MeUra mono-, di-, and trihydrates provides the possibility to study more complicated structures, such as base pairs. Recently[67] we have obtained preliminary results on low-temperature hydration of the Ade·Ura pair.

D. Comparison between Hydration in a Vacuum and in Solution

The results on hydration of nucleic acid bases in a vacuum, obtained by the MS method and described above, are related to the so-called hydrophilic or specific hydration. The inspection of peak intensities in the low-temperature mass spectra of hydrates can give some qualitative information about nonspecific interactions in the hydrates under investigation. A more detailed study of these two types of interaction can be performed by comparison of the data obtained in a vacuum with the enthalpies ΔH_{hydr} derived from the experimental values of solution and sublimation enthalpies, ΔH_{sol} and ΔH_{subl}, respectively. Recently[68,69] the values of ΔH_{sol} and ΔH_{subl} for Ura and Ade and their numerous alkyl derivatives have been measured by using a microcalorimeter, designed in the laboratory of Prof. Zielenkiewicz (Poland), and a low-temperature quartz resonator.[70] Hydration heats ΔH_{hydr} derived from the relationship

$$\Delta H_{hydr} = \Delta H_{solv}^{\infty} - \Delta H_{subl} \qquad (46)$$

involve two terms: (1) a positive one ΔH_{cav}, for the energy of a cavity formation in water, and (2) a negative one, ΔH_{int}, for the interaction energy of a biomolecule with its hydration shell. If one calculates the values of ΔH_{cav} according to Sinanoglu,[68,69] the values of ΔH_{int} for the interaction of all the water molecules in the hy-

dration shell of a biomolecule are readily obtained. From the values of ΔH_{int} and from the experimental hydration enthalpies of bases in a vacuum (Table VII), one can estimate the contribution of specific interactions to ΔH_{int} with the assumption of a 2-fold decrease of the energy of hydrogen bonds between water molecules and bases in aqueous solution caused by interactions between water molecules.[4] Thus, one obtains that in the case of *N*-methyladenines the ratio $\Delta H[M(H_2O)_3]/\Delta H_{int}[M(H_2O)_n]$ ranges from 0.19 (9MeAde) to 0.14 (6,6,9MeAde). In the case of 1,3MeUra $\Delta H[M(H_2O)_2]/\Delta H_{int}[M(H_2O)_n] = 0.21$. It can be seen that the contribution of specific interactions to the total hydration energy of Ade and Ura is as small as 15–20%. This estimation can be used for a more detailed interpretation of thermodynamic data on the hydration of biomolecules and their synthetic analogues in solution.[71]

V. Conclusion

The results presented above prove the utility of the method of TD-FIMS combined with its low-temperature modification for the investigation of thermodynamics of biomolecule interactions with each other and with solvent.

The main results on nucleic acid base complexes and their hydrates, obtained to date, can be summarized as follows:

1. The enthalpies of H-bonded and stacked dimers of nucleic acid bases have been measured in a vacuum. The data revealed a much greater stability of the Watson–Crick pairs as compared to homoassociation. The stability of base stacked dimers is about 30–40% lower than that for the Watson–Crick pairs.

2. Experimental and theoretical values for the enthalpies of water clusters $(H_2O)_n$ (n = 2–6) in a vacuum have been obtained. These results combined with quantum mechanical computations allowed us to propose cyclic configurations for water clusters with n = 3–6.

3. The enthalpies of multistep hydration of pyrimidine and purine methyl derivatives in a vacuum have been studied. In the case of Ura and Thy the strongest binding sites for the first and second water molecules are C(2)O and C(4)O. Cyt has three strong binding sites located in the polar part of the molecule between N(1)–H and NH_2. Ade also exhibits three active sites of hydration all round the molecule, the binding energy being, however, smaller than in the case of Ura and Cyt. The interaction enthalpy for the Gua·H_2O complex is the greatest as compared to those of all the other base monohydrates.

4. Higher water polymers $(H_2O)_n$ with n = 5–20 were observed by using a low-temperature FI ion source. The clusters with n = 8, 12, and 16 were shown to be the most stable. Base polyhydration was also achieved with the maximum number of water molecules in a cluster n = 10. The inspection of hydrate ion intensities confirmed the hydration schemes for nucleic acid bases described above.

Acknowledgments. I thank Prof. Zahradnik for giving me the opportunity to write this review and also Drs. Pyatigorskaya and Glukhova for their valuable assistance in the preparation of the manuscript.

VI. References

(1) Kyogoku, J.; Lord, R. C.; Rich, A. *Biochim. Biophys. Acta* **1969**, *179*, 10–17.
(2) Chem, M. C.; Lord, R. C. *Biochim. Biophys. Acta* **1974**, *340*, 90–94.
(3) Petersen, S. B.; Led, J. J. *J. Am. Chem. Soc.* **1981**, *103*, 5308–5313.
(4) Danilov, V. I.; Zakzhevskaya, K. M.; Zheltovsky, N. V. *Itogi Nauki Tekh., Ser. Mol. Biol.* **1979**, *15*, 74.
(5) *Intermolecular Interactions: From Diatomics to Biopolymers*; Pullman, B., Ed.; Wiley-Interscience: New York, 1979.
(6) Poltev, V. I. Thesis, Moscow State University, Moscow, 1985.
(7) Sukhodub, L. F.; Yanson, I. K. *Stud. Biophys.* **1976**, *59*, 209–220.
(8) Beckey, H. *Principles of Field Ionization and Field-Desorption Mass-Spectrometry*; Pergamon: London, 1977; p 335.
(9) Schulten, H.-R.; Monkhouse, P. B. *J. Biochem. Biophys. Methods* **1983**, *8*, 239–269.
(10) Schulten, H.-R.; Lattimer, R. P. *Mass Spectrom. Rev.* **1984**, *3*, 231–315.
(11) Karol, E.N.; Lobanov, V. V.; Nazarenko, V. A.; Pokrovsky, V. A. *Physical Foundations of Field Ionization Mass Spectrometry*; Naukova Dumka: Kiev, 1978; p 191.
(12) Sukhodub, L. F.; Yanson, I. K. *Dokl. Akad. Nauk SSSR* **1975**, *223*, 1010.
(13) Sukhodub, L. F.; Yanson, I. K. *Nature (London)* **1976**, *264*, 245–247.
(14) Yanson, I. K.; Teplitsky, A. B.; Sukhodub, L. F. *Biopolymers* **1979**, *18*, 1149–1179.
(15) Verkin, B. I.; Sukhodub, L. F.; Yanson, I. K. *Dokl. Akad. Nauk SSSR* **1976**, *228*, 1452.
(16) Verkin, B. I.; Yanson, I. K.; Sukhodub, L. F.; Teplitsky, A. B. *Biomolecular Interactions. Novel Experimental Approaches and Methods*; Naukova Dumka: Kiev, 1985; p 163.
(17) Langlet, J.; Claverie, P.; Caron, F.; Boeu, Vo. *Int. J. Quantum Chem.* **1981**, *19*, 299–338.
(18) Langlet, J.; Claverie, P.; Caron, F. In *Intermolecular Forces*; Pullman, B., Ed.; Reidel: 1981; pp 397–429.
(19) Sukhodub, L. F.; Tretyak, S. M.; Shelkovsky, V. S. Preprint, Institute for Low Temperature Physics and Engineering: Kharkov, 1985; p 12.
(20) Voet, D.; Rich, A. *Prog. Nucl. Acid Res. Mol. Biol.* **1970**, *10*, 183–264.
(21) Zhurkin, V. B.; Poltev, V. I.; Florentiev, V. L. *Mol. Biol. (Moscow)* **1980**, *14*, 1116.
(22) Sharafutdinov, M. R. Thesis, Institute of Biophysics, Puschino, 1984.
(23) Boiko, I. V.; Bublik, B. N.; Zinko, P. N. *Methods and Algorithms for Optimization Problems*; Vischa Shkola: Kiev, 1983; p 511.
(24) Deikalo, T. F.; Novikov, B. A.; Ruhlin, A. P.; Terehov, A. N. *Novel Software for ES Computers*; Finansi i Statistika: Moscow, 1984; p 207.
(25) Pohorille, A.; Burt, S. K.; MacElroy, R. D. *J. Am. Chem. Soc.* **1984**, *106*, 402–409.
(26) Förner, W.; Otto, P.; Ladik, J. *J. Chem. Phys.* **1984**, *86*, 49–56.
(27) Poltev, V. I.; Shulyupina, N. N. *J. Biomol. Struct. Dyn.* **1986**, *3*, 739–765.
(28) Pullman, A.; Perahia, D. *Theor. Chim. Acta* **1978**, *48*, 29–36.
(29) Pullman, B.; Miertus, S.; Perahia, D. *Theor. Chim. Acta* **1979**, *50*, 317–325.
(30) Poltev, V. I.; Shulyupina, N. N.; Dyakonova, L. P.; Malenkov, G. G. *Stud. Biophys.* **1981**, *84*, 187–194.
(31) Del Bene, J. E. *J. Comput. Chem.* **1981**, *2*, 188–189.
(32) Del Bene, J. E. *J. Chem. Phys.* **1982**, *76*, 1058–1063.
(33) Del Bene, J. E. *J. Comput. Chem.* **1983**, *4*, 226–233.
(34) Del Bene, J. E. *J. Mol. Struct.* **1984**, *108*, 179–197.
(35) Danilov, V. I.; Toloh, I. S. *Dokl. Akad. Nauk SSSR* **1984**, *274*, 968.
(36) Poltev, V. I.; Danilov, V. I.; Sharafutdinov, M. R.; Shvartsman, A. Z.; Shulypina, N. V.; Malenkov, G. G. *Stud. Biophys.* **1982**, *91*, 37–43.
(37) Danilov, V. I.; Sharafutdinov, M. R.; Malenkov, G. G.; Poltev, V. I. *Dokl. Akad. Nauk SSSR* **1982**, *268*, 485.
(38) Sharafutdinov, M. R.; Danilov, V. I. *Dokl. Akad. Nauk SSSR* **1983**, 76.
(39) Port, G. N. J.; Pullman, A. *FEBS Lett.* **1973**, *31*, 70–74.
(40) Beckey, H. D. *Z. Naturforsch., A: Astrophys., Phys. Phys. Chem.* **1960**, *15A*, 822–827.
(41) Schmidt, W. A. *Z. Naturforsch., A: Astrophys., Phys. Phys. Chem.* **1964**, *19A*, 318–327.
(42) Goldenfeld, I. V.; Nazarenko, V. A.; Pokrovsky, V. A. *Dokl. Akad. Nauk SSSR* **1965**, *161*, 861.
(43) Anway, A. R. *J. Chem. Phys.* **1969**, *50*, 2012–2021.
(44) Del Bene, J.; Pople, J. A. *J. Chem. Phys.* **1970**, *52*, 4858–4866.
(45) Kictemacher, H.; Lie, G. G.; Popkie, H.; Clementi, E. *J. Chem. Phys.* **1974**, *61*, 546.
(46) Lentz, B. R.; Scheraga, H. A. *J. Chem. Phys.* **1973**, *58*, 5296–5308.

(47) Owicki, J. C.; Shipman, L. L.; Scheraga, H. A. *J. Phys. Chem.* **1975**, *79*, 1794–1811.
(48) Vigasin, A. A. *Zh. Strukt. Khim.* **1983**, *24*, 116.
(49) Poltev, V. I.; Grokhlina, T. I.; Malenkov, G. G. *J. Biol. Struct. Dyn.* **1984**, *2*, 413–429.
(50) Sukhodub, L. F.; Verkin, B. I.; Shelkovsky, V. S.; Yanson, I. K. *Dokl. Akad. Nauk SSSR* **1981**, *258*, 1414.
(51) Sukhodub, L. F.; Telezhenko, Yu. V.; Shelkovsky, V. S.; Lisnyak, Yu. V. Preprint, Institute for Low Temperature Physics and Engineering, Kharkov, 1984; p 26.
(52) Starikovich, M. A.; Vigasin, A. A.; Yuchnevich, G. V. *Teplofiz. Vys. Temp.* **1976**, *14*, 739.
(53) Gebbie, H. A.; Burroughs, W. J.; Chamberlain, J. *Nature (London)* **1969**, *221*, 143–145.
(54) Dyke, T. R.; Muenter, J. S. *J. Chem. Phys.* **1972**, *57*, 5011–5012.
(55) Sukhodub, L. F.; Yanson, I. K.; Shelkovsky, V. S.; Wierzchowski, K. *Biophys. Chem.* **1982**, *15*, 149–155.
(56) Sukhodub, L. F.; Yanson, I. K.; Shelkovsky, V. S. *Stud. Biophys.* **1982**, *87*, 223–224.
(57) Sukhodub, L. F.; Shelkovsky, V. S. *Stud. Biophys.* **1985**, *107*, 35–42.
(58) Sukhodub, L. F.; Shelkovsky, V. S.; Wierschowski, K. L. *Biophys. Chem.* **1984**, *19*, 191–200.
(59) Peng, S.; Padva, A.; Lebreton, P. R. *Proc. Natl. Acad. Sci. U.S.A.* **1976**, *73*, 2966–2968.
(60) Padva, A.; O'Donnell, T. J.; Lebreton, P. R. *Chem. Phys. Lett.* **1976**, *41*, 278–282.
(61) Borodavkin, A. V.; Budovsky, E. I.; Morozov, Yu. V. *Itogi Nauki Tekh., Ser. Mol. Biol.* **1977**, *14*, 3.
(62) Sharafutdinov, M. R.; Danilov, V. I.; Poltev, V. I. *Dokl. Akad. Nauk SSSR* **1983**, *12*, 23.
(63) Clementi, E.; Corongiu, G. *J. Chem. Phys.* **1980**, *72*, 3979–3992.
(64) Gaivoronsky, D. A.; Sukhodub, L. F. *Prib. Tekh. Eksp.* **1983**, N 5, 173.
(65) Teplitsky, A. B.; Sukhodub, L. F. *Stud. Biophys.* **1986**, *111*, 153–154.
(66) Verkin, B. I.; Sukhodub, L. F.; Gaivoronsky, D. A. *Dokl. Akad. Nauk SSSR* **1984**, *277*, 1252.
(67) Sukhodub, L. F.; Teplitsky, A. B. *Stud. Biophys.* **1986**, *111*, 123–125.
(68) Teplitsky, A. B.; Glukhova, O. T.; Sukhodub, L. F.; Yanson, I. K.; Zielenkiewicz, A.; Zielenkiewicz, W.; Kosinski, J.; Wierzchowski, K. L. *Biophys. Chem.* **1982**, *15*, 139–147.
(69) Zielenkiewicz, A.; Zielenkiewicz, W.; Sukhodub, L. F.; Glukhova, O. T.; Teplitsky, A. B.; Wierzchowski, K. L. *J. Solution Chem.* **1984**, *13*, 757.
(70) Glukhova, O. T.; Shklyarevsky, O. I.; Yanson, I. K.; Teplitsky, A. B. *Zh. Fiz. Khim.* **1982**, *56*, 1535.
(71) Mrevlishvili, G. M. *Low Temperature Calorimetry of Biomolecules*; Metsniereba: Tbilisi, 1984; p 188.